

# **Automated Processing of ISIS Topside Ionograms into Electron Density Profiles**

Bodo W. Reinisch and Xueqin Huang  
University of Massachusetts Lowell  
Center for Atmospheric Research  
600 Suffolk Street, Lowell, MA 01854

and

Dieter Bilitza  
Raytheon ITSS, Code 632  
Greenbelt, MD 20771

and

H. Kent Hills  
QSS, 4500 Forbes Blvd  
Lanham, MD 20706

## **Final Report**

January 1999 to December 2001

No-cost extensions to December 2004

NASA Applied Information Systems Research

## CONTENTS

Summary	3
1.0 Introduction	4
2.0 The Digital Alouette/ISIS Ionograms	4
3.0 TOPIST Development	5
3.1 Basic Concepts	6
3.2 The interface for Ingesting ISIS Data	6
3.3 Reading Binary Input Data Files	8
3.4 Noise-filtering of Ionogram	9
3.5 Identification of Resonance and Cutoff Frequencies	12
3.6 Modeling the F Layer Peak	13
3.7 Automatic Scaling of Traces	13
3.8 O and X trace separation in ionograms with severe spread F	15
3.9 Inversion of Ionogram Traces to Electron Density Profiles	16
3.10 Recalculated Z Trace	16
3.11 Manual Scaling/Editing	17
3.12 Testing of TOPIST	21
4.0 Processing of Alouette and ISIS data	21
4.1 Alouette and ISIS Satellites and their Orbit Characteristics	21
4.2 Converting Existing NSSDC Data Sets to ASCII	24
4.3 TOPIST Processing of Digital Ionograms	26
5.0 References	28
APPENDIX A: Instructions for TOPIST Operations	30
APPENDIX B: An Example of the TOPIST Output File	33
APPENDIX C: Example of Processing Statistics by Year and Station	35
APPENDIX D: Papers presented	37
APPENDIX E: Papers published	38



## Summary

Modeling of the topside ionosphere has for the most part relied on just a few years of data from topside sounder satellites. The widely used Bent et al. (1972) model, for example, is based on only 50,000 Alouette 1 profiles. The International Reference Ionosphere (IRI) (Bilitza, 1990, 2001) uses an analytical description of the graphs and tables provided by Bent et al. (1972). The Alouette 1, 2 and ISIS 1, 2 topside sounder satellites of the sixties and seventies were ahead of their times in terms of the sheer volume of data obtained and in terms of the computer and software requirements for data analysis. As a result, only a small percentage of the collected topside ionograms was converted into electron density profiles. Recently, a NASA-funded data restoration project has undertaken and is continuing the process of digitizing the Alouette/ISIS ionograms from the analog 7-track tapes. Our project involves the automated processing of these digital ionograms into electron density profiles. The project accomplished a set of important goals that will have a major impact on understanding and modeling of the topside ionosphere:

- (1) The TOPside Ionogram Scaling and True height inversion (TOPIST) software was developed for the automated scaling and inversion of topside ionograms.
- (2) The TOPIST software was applied to the over 300,000 ISIS-2 topside ionograms that had been digitized in the framework of a separate AISRP project (PI: R.F. Benson).
- (3) The new TOPIST-produced database of global electron density profiles for the topside ionosphere were made publicly available through NASA's National Space Science Data Center (NSSDC) ftp archive at <nssdcftp.gsfc.nasa.gov>.
- (4) Earlier Alouette 1, 2 and ISIS 1, 2 data sets of electron density profiles from manual scaling of selected sets of ionograms were converted from a highly-compressed binary format into a user-friendly ASCII format and made publicly available through nssdcftp.gsfc.nasa.gov.

The new database for the topside ionosphere established as a result of this project, has stimulated a multitude of new studies directed towards a better description and prediction of the topside ionosphere. Marinov et al. (2004) developed a new model for the upper ion transition height (Oxygen to Hydrogen and Helium) and Bilitza (2004) deduced a correction term for the IRI topside electron density model. Kutiev et al. (2005) used this data to develop a new model for the topside ionosphere scale height (TISH) as a function of month, local time, latitude, longitude and solar flux F10.7. Comparisons by Belehaki et al. (2005) show that TISH is in general agreement with scale heights deduced from ground ionosondes but the model predicts post-midnight and afternoon maxima whereas the ionosonde data show a noon maximum. Webb and Benson (2005) reported on their effort to deduce changes in the plasma temperature and ion composition from changes in the topside electron density profile as recorded by topside sounders. Limitations and possible improvements of the IRI topside model were discussed by Coisson et al. (2005) including also the possible use of the NeQuick model.

Our project progressed in close collaboration and coordination with the GSFC team involved in the ISIS digitization effort. The digitization project was highly successful producing a large amount of digital topside ionograms. Several no-cost extensions of the TOPIST project were necessary to keep up with the pace and volume of the digitization effort.

## 1.0 Introduction

The goal of this project is to produce a reliable database for the electron density distribution in the Earth's topside ionosphere. Current models of the topside global electron density distribution are highly speculative because of the lack of sufficient measured data. Millions of topside ionograms had been measured with the Alouette 1, 2, and ISIS 1, 2 satellites in the sixties and seventies (Jackson, 1986) but only a tiny fraction had been converted into electron density profiles, because the topside ionograms had to be manually scaled. A recent AISRP-funded data restoration effort has succeeded in digitizing over 300,000 of the analog ISIS-2 ionograms as a first step towards a full analysis of this important data set. The goal of our project is to develop software for the automated scaling and inversion of digital ionograms and then to apply this software to the analysis of the large volume of digitized ionograms.

## 2.0 The Digital Alouette/ISIS Ionograms

The Alouette/ISIS topside sounders were ionosondes transmitting short radio pulses with frequencies scanning from 0.1 to 20 MHz. (Jackson et al., 1980). The transmitted electromagnetic waves propagate into the ionosphere until they are reflected at the location where the plasma frequency  $f_N$  equals the wave frequency  $f$  (for the ordinary mode). The square of the plasma frequency is proportional to the electron density  $N$  ( $fN^2 = 80.6 N$ ,  $fN$  in Hz and  $N$  in  $m^{-3}$ ). The sounder measures the echo propagation time  $t_p$  at all the sounding frequencies for which echoes are received. Figure 1 shows examples of ISIS-2 ionograms plotted on CDAWeb (<http://cdaweb.gsfc.nasa.gov>). Displaying the echo amplitudes as a function of echo propagation delay and frequency produces an ionogram. The ionogram images generally extend from 0.1 to 20 MHz along the horizontal frequency axis, and from zero to 3000 km along the vertical apparent or "virtual" depth axis. The virtual depth (or range) is defined as  $R' = 0.5 c t_p$  ( $c$  = speed of light). A color code is used to indicate different amplitude levels. The ionograms show different echo traces resulting from the so-called O, X, and Z modes of propagation (Hagg et al., 1969; Budden, 1985, Fig.13.6). In addition, a number of "resonance spikes" generally occur that extend with decreasing amplitudes to large virtual depth within a narrow frequency band. The resonance frequencies at the center of the spikes are functions of the magnetoplasma conditions at the location of the satellite (e.g. Muldrew, 1969, 1972).

The digitized ionogram data are archived at the National Space Science Data Center in a full-resolution and an average form (<http://nssdcftp.gsfc.nasa.gov>). The full-resolution ionograms consists of 8-bit receiver-amplitude values collected at a 40 kHz rate (3.75 km virtual range increments). Each data file contains the time and the frequency associated with each sounder pulse. In addition, the file includes orbit information (date, time, latitude, longitude, altitude, dip, L-value, etc.). The average ionograms have a similar format as the full ionograms but each receiver-amplitude value represents the average of 4 of the 40 kHz 8-bit values (15 km range increments). A detailed format description for the full and average files can be found at [http://nssdc.gsfc.nasa.gov/space/isis/des\\_av.html](http://nssdc.gsfc.nasa.gov/space/isis/des_av.html). The full and average ionogram data are stored in OSII binary format; the average ionograms are also available in Common Data Format (CDF). The CDF data are also available for plotting, browsing, and downloading from the Space Physics Data Facility (SPDF) CDAWeb system (<http://cdaweb.gsfc.nasa.gov>). We have used the full-resolution ionograms for our project to provide the maximum available information to the autoscaling task.

ISIS-2 QUI>Quito AV>Average Ionogram

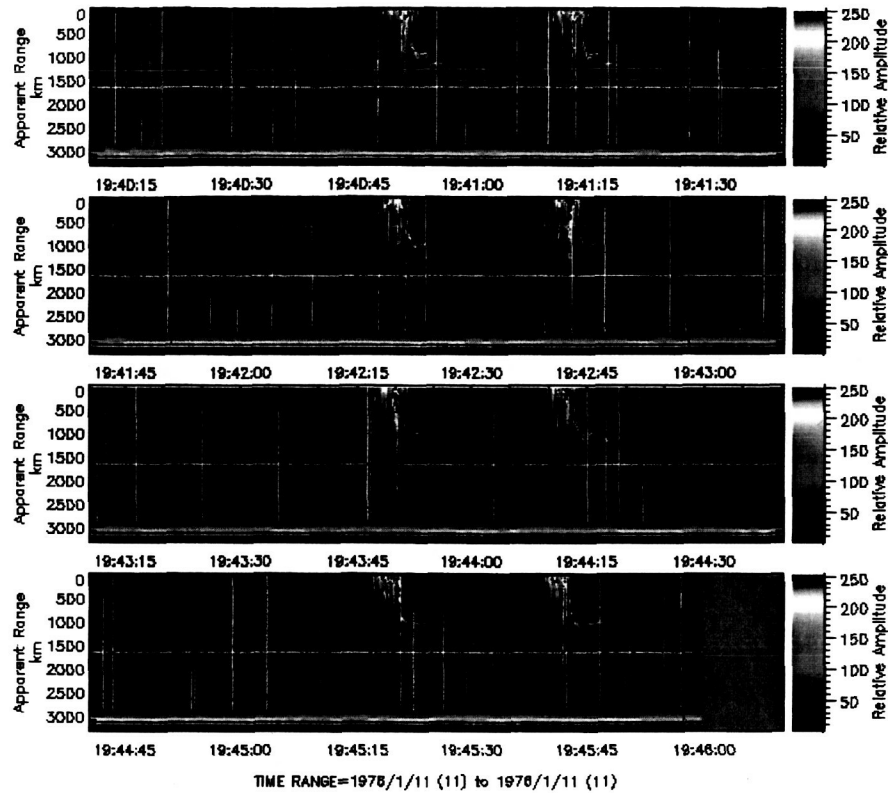


**Figure 1.** Examples of ISIS-2 topside ionograms as displayed by CDAWeb.

Ionograms can be very complicated showing broadened echo traces, so-called spread F that is caused by irregularities in the electron density distribution, and ducted echoes with long delay times (Muldrew, 1969). The automatic processing will not always be able to identify the vertical O and X traces and the resonance frequencies for such highly disturbed ionograms.

### 3.0 TOPIST Development

As part of our project we have developed the TOPside Ionogram Scaling and True height inversion (TOPIST) software for the automated scaling and inversion of digital topside ionograms. In the following section we discuss the different elements of this development effort. The first and main task is to develop algorithms that automatically identify the vertical echo traces and the plasma resonance frequencies in the “ionogram image” and extract the leading edges of the echo traces. The so-called virtual range as function of frequency,  $R'(f)$ , in combination with the plasma resonances can then be inverted to  $N(h)$  profiles (Reinisch and Huang, 1982, 1983; Huang and Reinisch, 1982).

### 3.1 Basic Concepts

For the trace identification, neural network techniques could be considered. But based on our experience (Galkin et al., 1996) a knowledge-based retrieval system that simulates the way an expert human scaler proceeds is superior and was therefore used in our work following earlier studies by Reinisch and Huang (1982, 1983). One of the difficulties in scaling analog ionograms is to distinguish the O and X mode traces. The general theory of radio wave propagation in a magnetoplasma must be used to identify these two traces since the data do not show the wave polarization. Knowing the resonance frequencies  $fN_s$  and  $fX_s$  can be helpful in identifying the O and X traces since they are the starting points for the  $R'_O(f)$  and  $R'_X(f)$  traces at  $R'=0$ . Once the two traces are identified, a leading edge algorithm can determine the leading edges of the echo traces which are required as input for the profile inversion. Sometimes part of the O or the X trace is missing and it is therefore advantageous to make use of both traces to calculate  $N(h)$  (Huang and Reinisch, 1982).

We divided the development of an automatic scaling routine into three main tasks: (1) reading the digital ionograms, (2) autoscaling the ionogram traces and resonance frequencies, and (3) calculating the electron density profile with a true height inversion algorithm. This includes the following sub-tasks:

- Reading/Checking Data File
- Noise Filtering
- Identifying Resonance/Cutoff Frequencies
- Calculating the F2-Layer Peak
- Automatic Echo Trace Scaling
- Manually Assisted Scaling
- Profile Inversion
- Creating Output
- Ionogram Display

The flow chart in Figure 2 illustrates the TOPIST processing of the digital ISIS ionograms and shows the logical relations of the various parts in TOPIST.

The TOPIST program was developed on a PC system using Windows 95/98 or Windows NT as the platform and Visual Fortran as the compiler. For the ingestion of the digital ISIS ionograms, a very elaborate interface was designed that serves during the TOPIST development and will be helpful to other users of the ISIS raw database. The results of the different processing steps are graphically displayed and all the figures can be saved. All scaled trace data and the inverted electron density profiles are stored in ASCII formatted files.

### 3.2 The Interface for Ingesting ISIS Data

TOPIST provides an interface to communicate with the user. The user can specify the data files to be processed, select the execution mode, etc. as shown in Figure 3. The user specifies the following items:

**DATA TYPE/FORMAT OF THE INPUT FILES:** The current TOPIST can only accept binary coded data files.

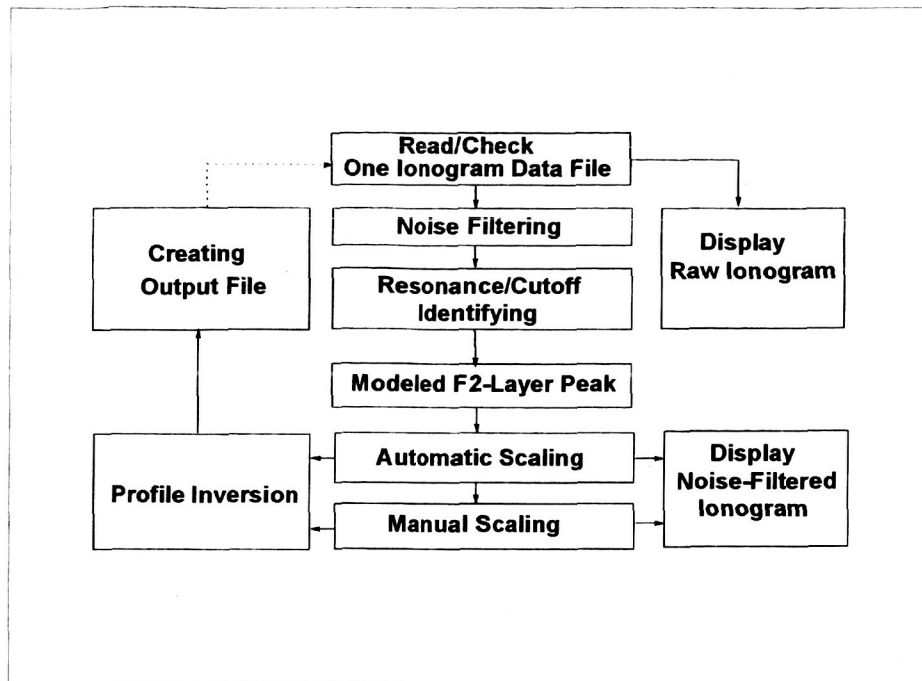


Figure 2. Flow Chart of TOPIST.

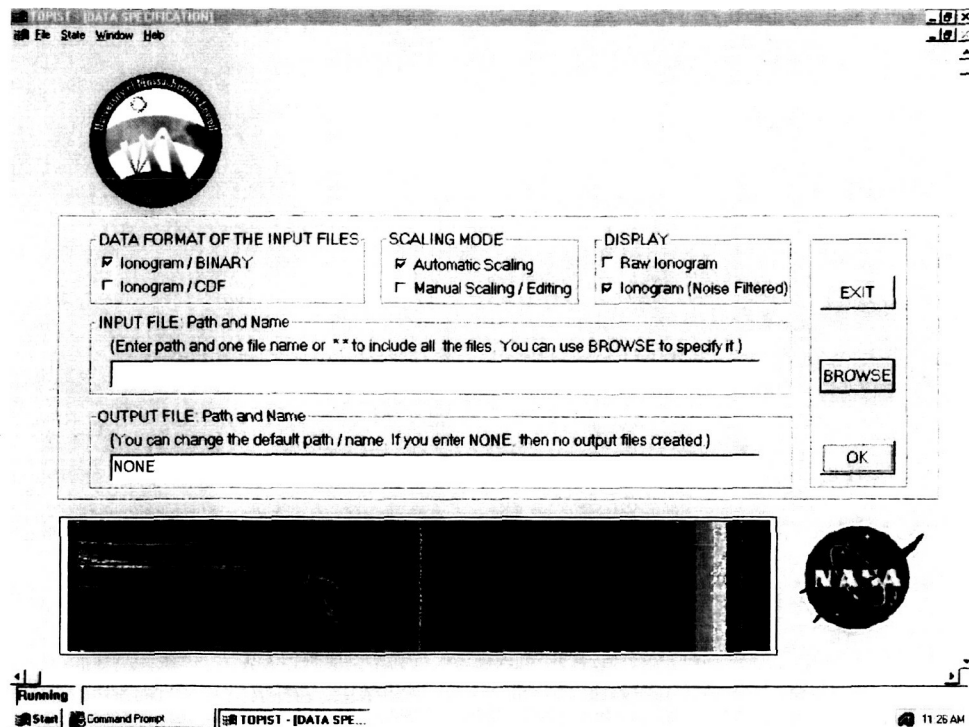


Figure 3. TOPIST main interface window.

IONOGRAM SCALING MODE: The user has two options. Automatic Scaling (default) or manually editing the scaling. Since topside ionograms can be very complicated it is impossible

to develop an algorithm that can auto-scale all ionograms with good accuracy. A second option is therefore provided, called “Automatic Scaling + Manual Editing”. This option allows the user to manually edit the scaling if the autoscaling is not satisfactory.

**DISPLAY:** The ionograms can be displayed in two different ways, either without noise filtering (Raw Ionogram), or with noise filtering. There is also the option to superimpose the scaled traces and the electron density profile on the displayed ionogram. As it takes more time to display raw ionograms, the noise-filtered ionograms are the default option.

**INPUT and OUTPUT FILE:** The data files to be processed are assumed to reside in a subdirectory of the processing computer. The user can enter the path and name of one input data file. The output file will automatically be stored in the same subdirectory and its name is the same as the input file but with the extension “.TOP”. Wildcard entry can be used to process all or a group of files in a selected directory. The user can also activate the BROWSE window to search or specify the data files. Figure 4 shows an example with 14 data files in drive D: in the subdirectory /ISIS\_DATA/DATA1/. The selections can be made in arbitrary order and modified at any time before pushing the OK button to initiate a TOPIST run.

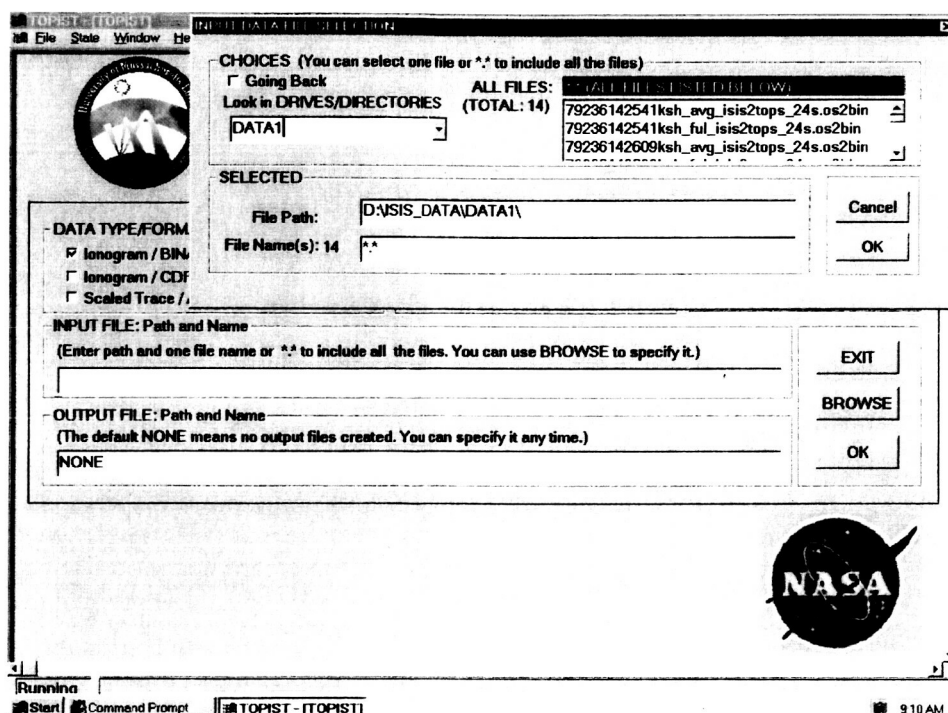


Figure 4. File browser.

### 3.3 Reading Binary Input Data Files.

When reading a data file, a box in the MESSAGE window indicates what percentage of the file has been read successfully as illustrated in Figure 5. If format errors are found while reading a file, TOPIST disregards the file and proceeds to read the next file.



```

IONOGRAM DATA
DATA FORMAT: EIMAFY
INPUT FILE: D:\ISIS_DATA\DATA1\79236142541KSH_AVG_ISIS2TOPS_24S.OS2BIN
OUTPUT FILE: NONE
SCALING MODE: AUTOMATIC SCALING

THE PROGRAM IS READING DATA FILE. PLEASE WAIT...

```

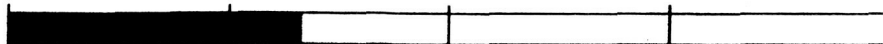


**Figure 5.** Status display during data reading.

The processing results, including the coordinates of the original ionogram, the resonance frequencies, the auto-scaled O- and X-traces, and the electron density profile are all stored in an ASCII file. The data format uses the SAO format specifications (Reinisch, 1998) standardized for bottomside ionograms. In order to check the processing quality, TOPIST can read these files and superimpose the traces and the profile on the displayed ionogram.

### 3.4 Noise-filtering of Ionogram.

When displaying of RAW IONOGRAMS has been selected, the raw ionogram is shown in the RAW IONOGRAM window. The frequency scan ionograms are generally preceded by a fixed-frequency measurement. These two ionogram parts are displayed on two separate pages as illustrated in Figures 6a,b. TOPIST suppresses the noise for both the fixed frequency part and the swept-frequency part and forms a new data set for further processing. Figure 6c shows the noise-filtered swept-frequency ionogram.

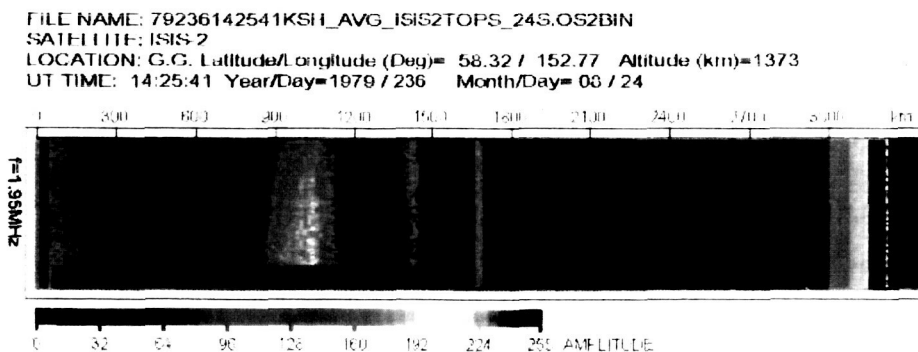


**Figure 6a.** Full-resolution digital ISIS ionogram: Fixed-frequency part.

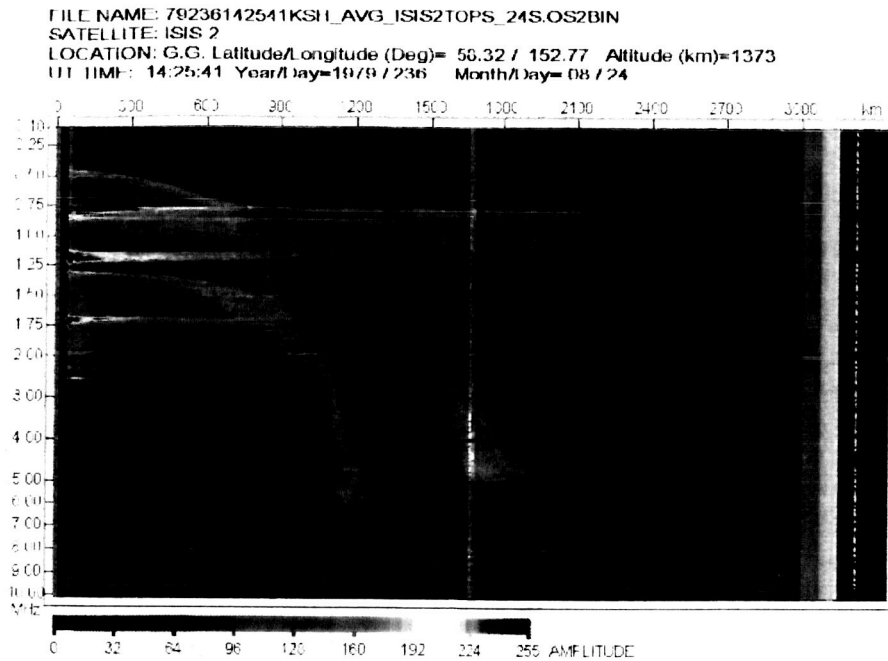


**Figure 6b.** Full-resolution digital ISIS ionogram: Swept-frequency part. The black trace near  $R' = 2,700$  km represents the automatic gain control.

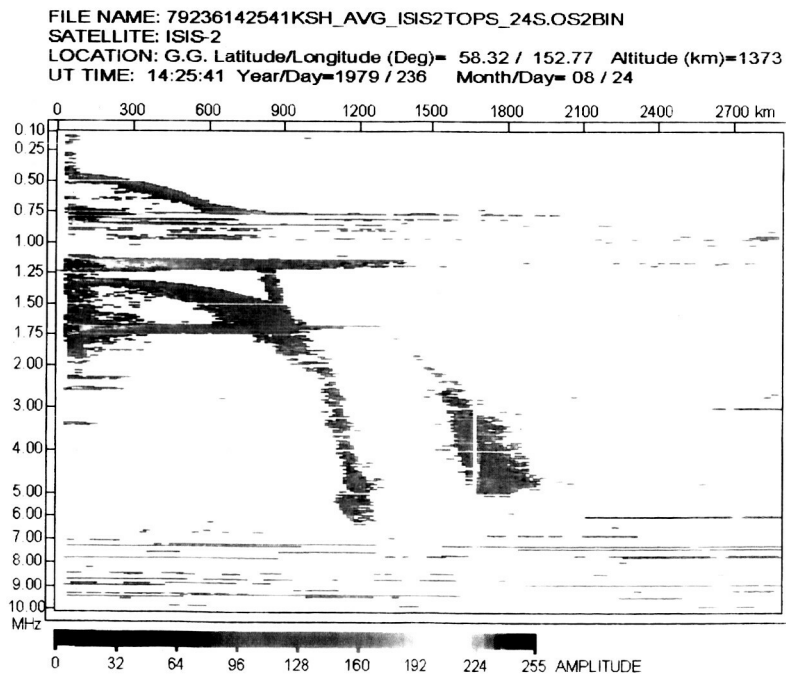


**Figure 6c.** The effect of noise filtering.



The noise filtering is done independently for each frequency line. The linear amplitude values range from 0 to 255. The amplitude values for each frequency line are sorted into 16 equally sized boxes to find the distribution of amplitudes. The most probable amplitude (MPA) is determined and all amplitudes smaller than  $AMP_{noise} = 1.5 \text{ MPA}$  are reset to zero. Since this procedure could suppress the resonance spikes,  $AMP_{noise}$  is defined as  $AMP_{noise} = \text{Smaller}(AMP_{noise1}, AMP_{noise2})$  where  $AMP_{noise1}$  and  $AMP_{noise2}$  are the noise levels of the closer and more distant ranges. Figure 7a illustrates the noise filtering process for a

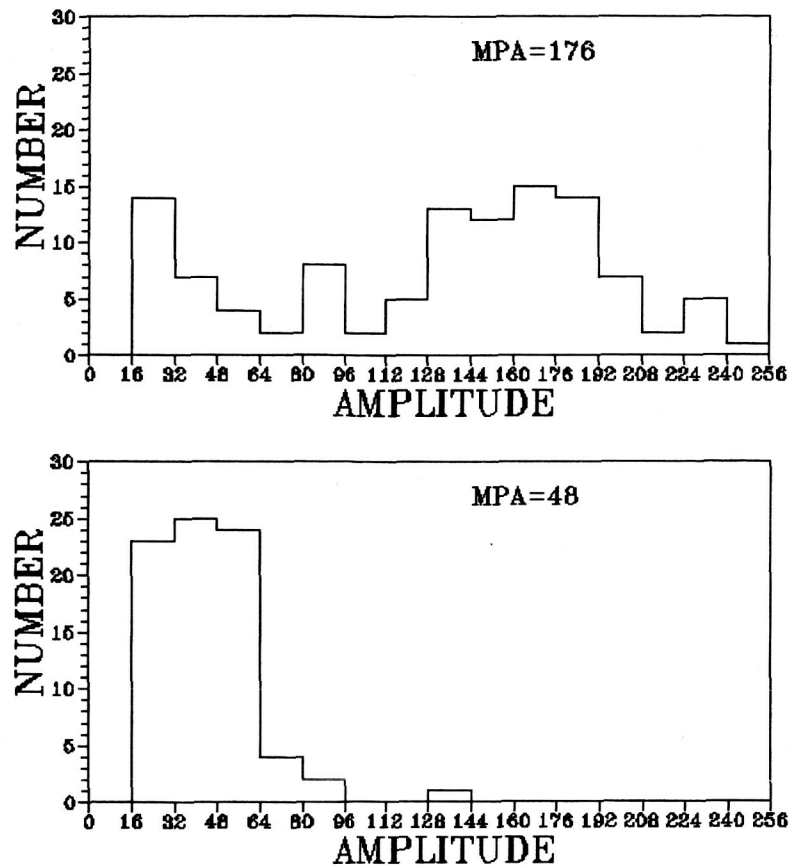


**Figure 7a.** Amplitude histograms for near (top) and far (bottom) ranges: For frequency with a resonance spike.

frequency line in the resonance region. The upper panel represents the amplitude distribution for the near ranges. The high MPA of 176 is the result of a resonance spike.  $MPA_{noise}$  is determined from the lower panel for the far ranges as  $MPA_{noise} = 1.5 \times 48 = 72$ . Any image bin in the frequency line with amplitude less than 72 will be suppressed. The amplitude histograms in Figure 7b are typical for a frequency with echo traces but no resonance spikes. Any image bin in the frequency line with amplitude less than 96 will be suppressed.

The auto-scaling procedure uses the noise-filtered ionogram. This approach is similar to the one used by the ARTIST software in the ground-based Digisondes (Reinisch, 1996).

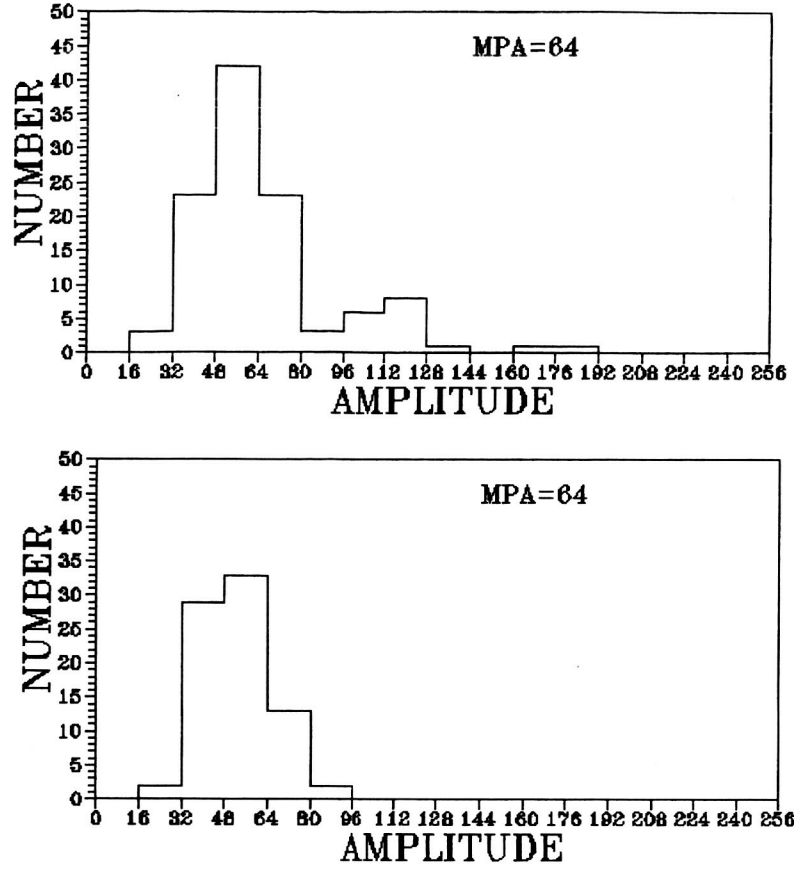


**Figure 7b.** Amplitude histograms for near (top) and far (bottom) ranges: For frequency with echo trace but no resonance spike.

### 3.5 Identification of Resonance and Cutoff Frequencies.

The algorithm for identifying resonance and cutoff frequencies is based on the method developed by (Reinisch and Huang, 1982). The algorithm searches only for the significant resonance and cutoff frequencies that are typically observed on ionograms. The relations of the gyrofrequency  $fH$ , the plasma frequency  $fN$  (the O trace cutoff frequency), and the upper hybrid frequency  $fT$  to one another and to the X and Z cutoff frequencies,  $fX$  and  $fZ$ , are given as

$$\begin{aligned} fN_s^2 &= fZ_s^2 + fZ_s \cdot fH_s \\ fT_s^2 &= fH_s^2 + fZ_s^2 + fZ_s \cdot fH_s \\ fX_s &= fH_s + fZ_s \end{aligned} \quad (1)$$

The gyrofrequency at the satellite position,  $fH_s$ , is calculated from the satellite coordinates using a geomagnetic model. Selecting  $fZ_s$  as a free variable, the above relations determine  $fN_s$ ,  $fT_s$ , and  $fX_s$ . A five frequency-comb window is constructed for a set of testing values of  $nfH_s$ ,  $fN_s$ ,  $fT_s$ ,  $fX_s$  and  $(n+1)fH_s$ , where  $n$  is chosen such that  $nfH_s$  and  $(n+1)fH_s$  are as close as possible to the other three frequencies. Each comb frequency is made three frequency steps wide and all amplitudes within the comb window are summed. Sliding this comb window along the frequency axis and searching for the maximum amplitude sum determines  $fZ_s$ ,  $fN_s$ ,  $fT_s$  and  $fX_s$ .

The identified resonance and cutoff frequencies  $fZ_s$ ,  $fN_s$ ,  $fT_s$ ,  $fX_s$ , and  $fH_s$ ,  $2fH_s, \dots, (n+1)fH_s$  are marked on the noise-filtered ionogram in Figure 7. The algorithm was tested with hundreds of ionograms and was found to perform with high accuracy. For a few ionograms, when the algorithms performed badly, the modeled gyrofrequency was incorrect. This problem needs further investigation.

For most cases, this algorithm gives very good identification. However, the tests show that for about 20% of the ionograms the correct positions of the resonance/cutoff frequencies should be the location of the second maximum not the first or, for a few cases, the third maximum. So the algorithm was modified to work the following way: Three sets of resonance/cutoff frequencies are determined with the sliding comb window method. After the trace points are identified, profile inversion is applied sequentially using the three sets. The set that provides the best agreement between the recalculated O and X traces and the observed ionogram traces is selected for the output file.

### 3.6 Modeling the F Layer Peak.

According to the sounding time of the ionogram given in the data file, the 12-month smoothed sunspot number is determined. Using the URSI (Rush et al., 1989) or CCIR (CCIR, 1966) coefficients, the critical frequency and the peak height of the F layer are calculated. We are using this modeled F layer peak to assist in the autoscaling of the O and X traces. In Figure 8, the modeled F layer peak is marked at  $fmP = 5.32$  MHz and  $RmP = 1,139$  km.

### 3.7 Automatic Scaling of Traces.

To determine the trace points and identify their wave mode, O or X, the algorithm takes a series of steps.

**3.7.1 Determination of the baseline.** This procedure finds the approximate location of the echo traces searching from  $fN_s$  to the last sounding frequency. For each frequency  $i$  a range  $R_i$  is calculated as

$$R_i = \frac{\sum A_j \cdot R_j}{\sum A_j} \quad (2)$$

where  $A_j$  is the amplitude at range  $R_j$ . The baseline points  $R_i$  usually end up between the O and X trace points or around one of them for frequencies with echoes, while for frequencies beyond the trace region or in the gaps of traces they distribute randomly. Interpreting the baseline from  $fN_s$  to the modeled  $foF2$  as the approximate echo trace, a preliminary profile is calculated. An echo trace is then calculated from this profile to replace the original baseline. This new baseline is smooth and is a more reliable guide for the determination of the trace points.

**3.7.2 Determination of a separation line.** This process tries to separate the O and X echoes. For each frequency, two  $R_i$  are determined, one above,  $R_{ia}$ , and one below the baseline,  $R_{ib}$ . In general, these are the O and/or X echoes that may be separated by several range bins, or may be very close together where the O and X traces merge. A separation line is defined by  $S_i = (R_{ia} + R_{ib})/2$ .

**3.7.3 Identification of O and X traces.** The wave mode of a trace point is determined using trace continuity arguments and considering its location with respect to separation line.

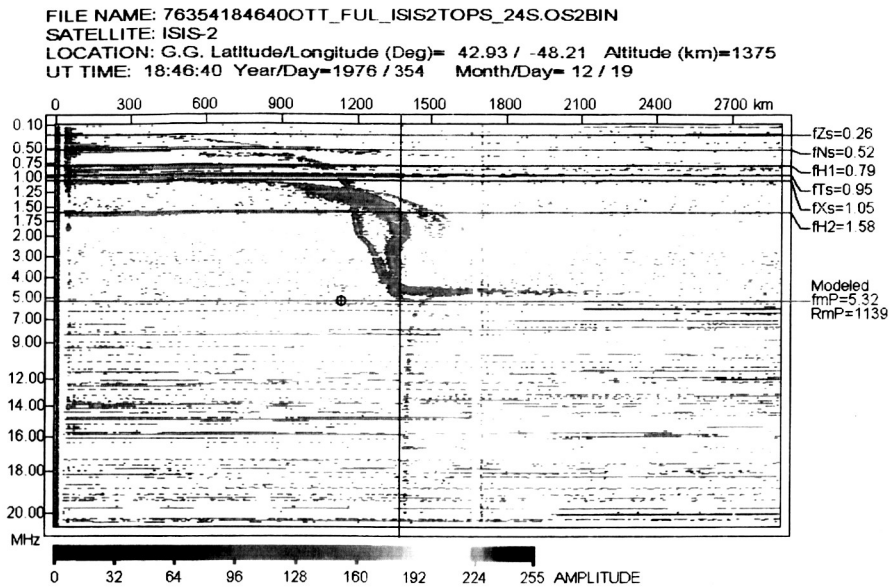


**Figure 8.** A five-frequency comb window determines six resonance frequencies shown on top of the ionogram. The red circle at 5Mhz and 1150 km indicates the URSI prediction of the F2 layer peak.

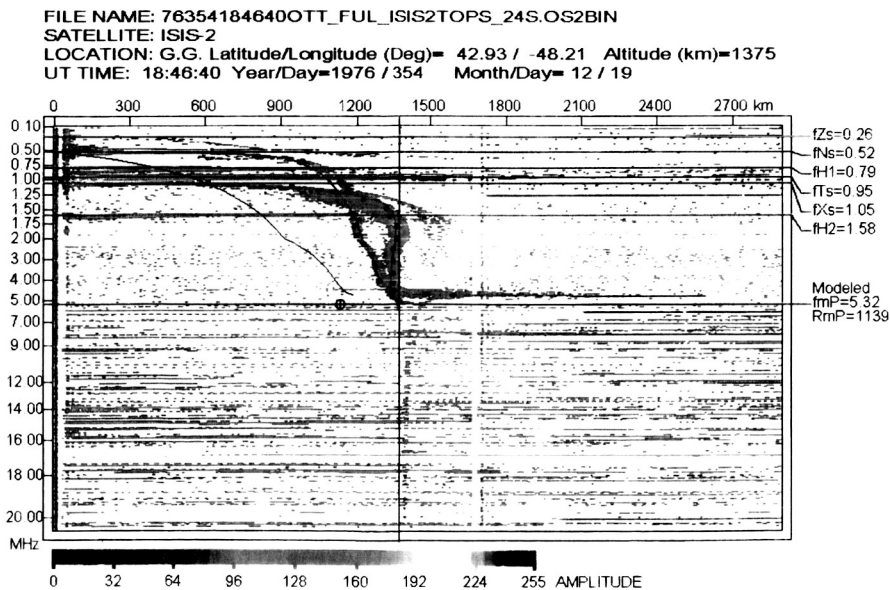


**Figure 9.** TOPIST scaling of the O trace (red line) and X trace (green line), and the topside electron density profile (black line) calculated from the satellite altitude to hmF2. The dots on the traces denote the manually scaled trace points.

**3.7.4 Determination of the trace cusps.** This procedure determines foF2 and fxF2. The algorithm first searches for ground returns. In their presence it is relatively easy to find the cusps of the O and X traces. In the absence of ground returns, the initial foF2 value, found at the end of the O cusp, is varied until the recalculated trace best reproduces the ranges of the measured O echoes. This best fit is defined as the maximum sum of all amplitudes on the recalculated trace. For ionograms without a well-defined cusp the modeled F layer peak coordinates are used. An example of an ionogram with a strong O cusp and a weak X cusp is shown in Figure 9. The auto-scaled O (red line) and X (green line) traces are shown. The red and green dots on the traces are manually scaled trace points. Also shown is the electron density profile (black line) calculated from the auto-scaled traces.

### 3.8 O and X trace separation in ionograms with severe spread F.

Unlike for the proposed modern topside sounders (Reinisch et al., 2001) there is no tagging of echoes with different polarizations in the ISIS ionograms, and the most difficult task in the automatic scaling is the identification of the O and X trace points. There are distinct O and X traces in many ionograms for which it is not difficult to identify O and X trace segments although ambiguities occur around the crossing points. The task for successful automatic scaling is to decide which trace segments are part of the O trace, which are part of the X trace, and to overcome the difficulty of the trace crossing ambiguity. Starting from any assumed combination of O and X trace segments, a profile inversion is done and the cross points for the recalculated O and X traces are determined. Then the O and X trace segment identifications are adjusted according to the calculated cross points. The adjustment procedure is repeated until the recalculated O and X traces best agree with the assumed combination of O and X trace points. Unfortunately, it is difficult to do the proper trace segmentation in the presence of severe spread. We have augmented the initial procedure to improve the algorithm. When the parabolic fitting method used for the segmentation of the trace points ends up with unsatisfactory results (recalculated traces not reproducing the measured traces), one of the generic functions shown in Figure 10 is used to fit the first part of the ionogram trace starting at the resonance frequency (0

$$R = R_0 - \{ [R_0 + DR] \cdot \exp[-\alpha \cdot (f - f_0)] - DR \cdot \exp[-\beta \cdot (f - f_0)] \}$$

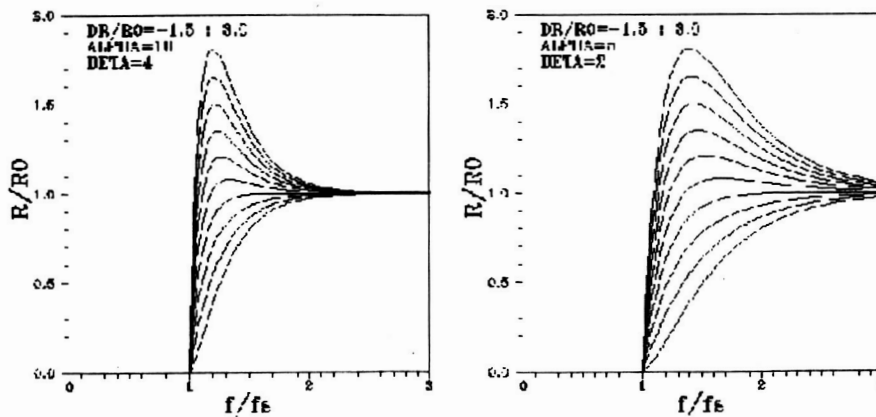


Figure 10. Generic function used to fit the first parts of the O and X traces.

range). It is initially assumed that this is an O trace, and the profile is calculated with this assumption. The recalculated O and X traces are compared with the measured trace segments, and the coefficients in the generic functions are optimized to obtain a best fit. Iteration is required to complete the scaling.

### 3.9 Inversion of Ionogram Traces to Electron Density Profiles.

Well-established techniques exist for the inversion of the  $R_O'(f)$  and  $R_X'(f)$  traces to  $N(h)$  profiles (Jackson, 1969; Jackson et al., 1980; Titheridge and Lobb, 1977). A specialized technique for inverting autoscaled traces, which may contain erratic jumps in the virtual depth, had been developed and tested by Huang and Reinisch (1982). This program used both the O and X traces, or segments thereof, to calculate the "true" height profile  $N(h)$  from the satellite altitude to the peak height of the F2 layer. This inversion program was adapted for the processing of the ISIS data.

We are using the inversion algorithm developed for automatically scaled ionograms by Huang and Reinisch (1982). The profile is represented in terms of shifted Chebyshev polynomials  $T_i^*(g)$

$$R = R_m + g^{1/2} \sum_{i=0}^I A_i T_i^*(g) \quad (3)$$

with

$$g = \frac{\ln(fN / fN_m)}{\ln(fN_s / fN_m)}. \quad (4)$$

Here  $fN$  is the plasma frequency at the radial distance  $R$ , measured from the satellite, and  $fN_s$  and  $fN_m$  are the plasma frequencies at the satellite position and at the F layer peak, respectively. The profile inversion is done by a least-squares fit using either the O or X trace points, or both. There is very little requirement for the trace smoothness and spacing of the points. The variation of the gyrofrequency with height is included assuming a cubic law dependence; the dip angle variation with height is ignored since its effect on the profile inversion is minute.

Figure 11 shows the topside electron density profile calculated from the auto-scaled traces of the ionogram in Figure 9. The profile is plotted versus plasma frequency (top) and electron density (bottom). To verify the accuracy of the auto-scaling and the profile inversion, we compared the TOPIST profile with the profile obtained manually by R.F. Benson (GSFC) and shown as dashed line in Figure 11. This was obtained by manually scaling the ionogram (see the dots on the traces in Figure 9) and by applying the Jackson (1969) inversion routine. The agreement is extremely good. The small differences in the profile at ranges close to the satellite are the result of different  $fN_s$  values. The slightly higher TOPIST value is likely the more accurate one considering TOPIST's special technique used to find the resonance frequencies.

### 3.10 Recalculated Z Trace.

After profile inversion, the Z trace is calculated. Figure 12 shows the recalculated Z trace with a cutoff frequency of 1.07 MHz.

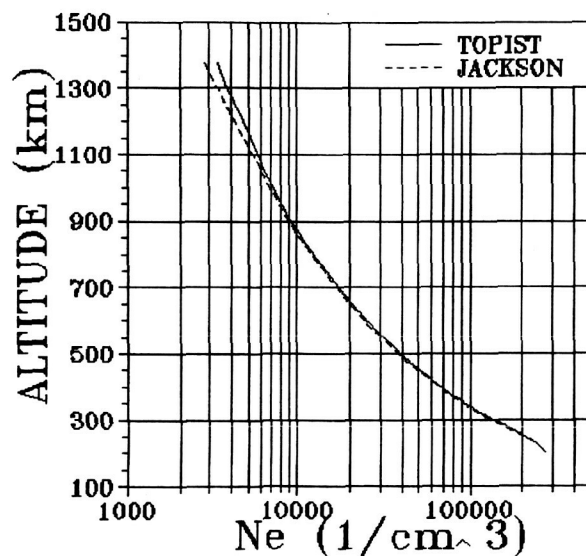
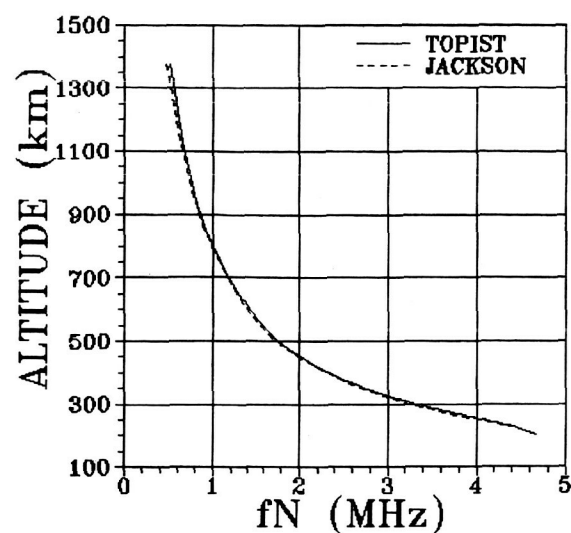


**Figure 11.** Comparing the automatic profile (solid line) with the manual profile (dashed line). The profiles are plotted as function of plasma frequency (top) and electron density (bottom).

### 3.11 Manual Scaling/Editing.

The objectives of the manual scaling/editing are:

- To check the results of the automatic scaling;
- To do manual scaling if the result of the automatic scaling for an ionogram is not satisfactory; and
- To do manual scaling for those ionograms for which high accuracy is required.

For manual scaling, *Manual/Editing Scaling* has to be selected as scaling mode. If the *Automatic Scaling* is also selected, TOPIST will do automatic scaling first and then show the identified



resonance/cutoff frequencies, O and X traces, and the inverted profile, etc., superimposed on the noise-filtered ionogram as illustrated in Figure 13a. The main task of the manual scaling for this

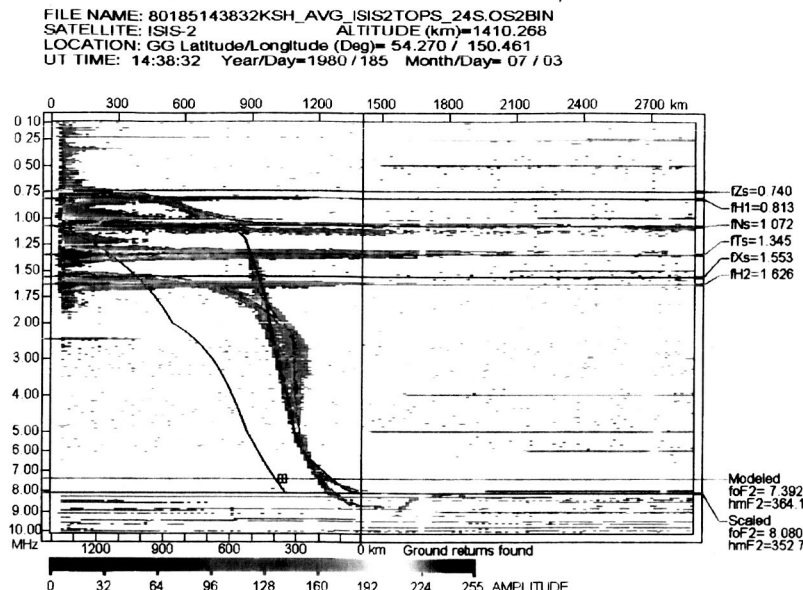


**Figure 12.** Example for automatic scaling: the scaled resonance/cutoff frequencies, traces, inverted profile and recalculated traces are shown in the noise-filtered ionogram.

example seems to be to correct the resonance/cutoff frequency positions. If the *Automatic Scaling* was not selected, and if no manual scaling was done before for an ionogram, the manual scaling will start with the display of the noise-filtered ionogram. Figure 13a shows this case, in which no trace scaling was done before, but the resonance/cutoff frequencies were automatically (and correctly) identified.

Operational scaling instructions are given when clicking on a specific task. A mouse click on a box can select any one of the scaling items: *O-TRACE*, *X-TRACE*, and *foF2/RESONANCE LINES* (Figures 13a and 14a).

- To scale the O-trace, the box *O-TRACE* should be selected and it will be highlighted. The trace can be drawn by moving the cursor while the mouse left button is held down. The points of the O-trace will be erased if the mouse right button is held down. The scaled trace need not be continuous. Some trace gaps could be filled by interpolation or extrapolation. However, this is not recommended unless the scaler is very sure about the trace extension.
- The same can be done for the X-trace when the box *X-TRACE* is selected.
- The resonance/cutoff frequencies can be corrected when the box *foF2/RESONANCE LINES* is selected. Placing the cursor on any of the identified frequency lines and dragging it to the required position, while holding the left button of the mouse down, can accomplish this. The values of the resonance frequencies are physically related and when one of them changes, the others will change automatically. The scaling of O-trace, X-trace and resonance/cutoff frequency lines can be done in any order and repeated again if necessary.



- When the trace image occupies a small part of the screen, the box “ZOOM IN/OUT” appears. Pushing the box once or several times enlarges the image occupancy as has been done in Figure 14b.

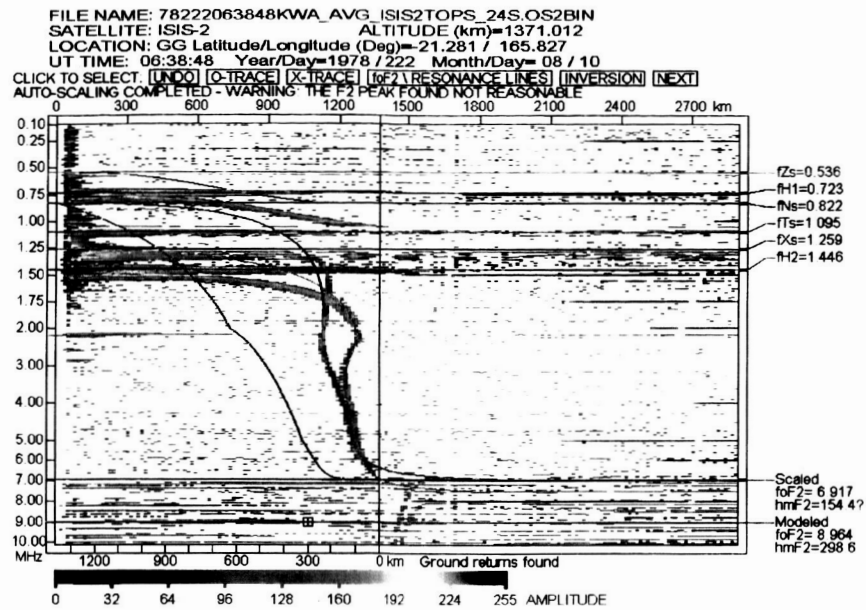


Figure 13a. Example of wrong automatic scaling for resonance/cutoff frequencies.

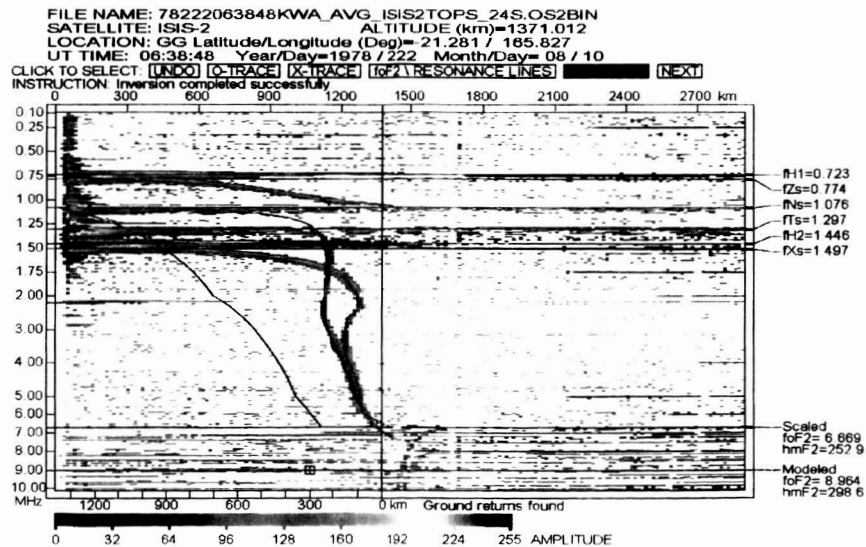
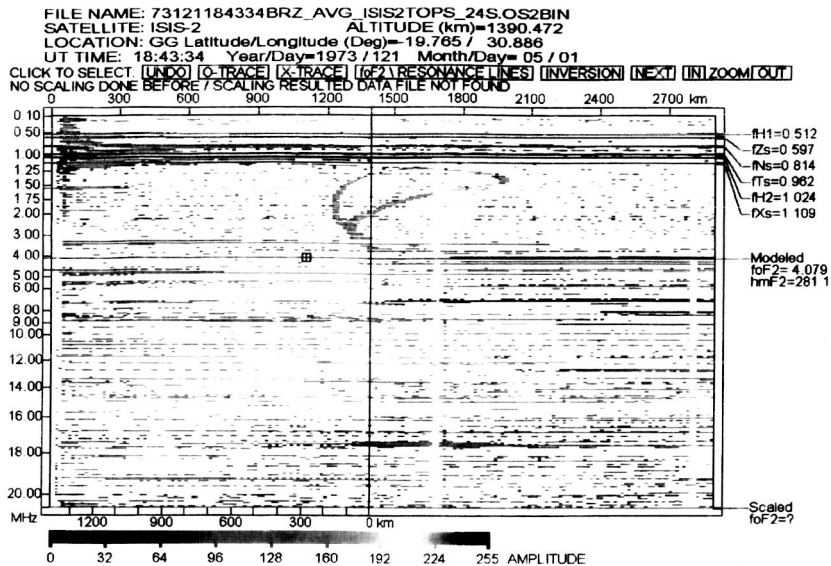
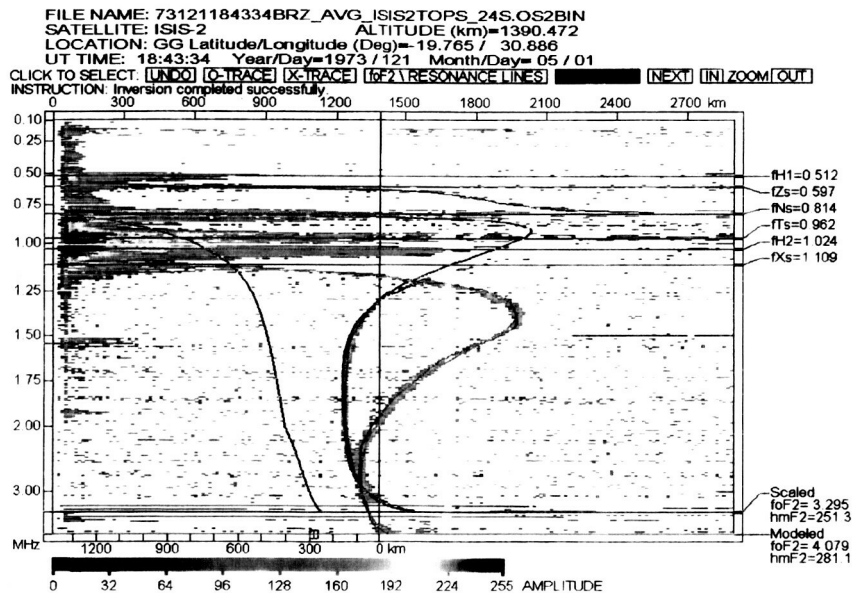


Figure 13b. Result of manual scaling of the ionogram in Figure 13a.



**Figure 14a.** Example without automatic scaling.



**Figure 14b.** Result of manual scaling of ionogram in Figure 14a.

- The selection of the box *INVERSION* will initiate the profile inversion program using the scaled traces and the identified resonance/cut off frequencies. The profile will be superimposed on the ionogram display if the inversion was successful. When it fails, the reason is shown.
- The above procedures are repeated to refine the scaling until a satisfactory result is obtained. Then the box *Next* should be clicked to display the next ionogram. At this time the scaling and inversion results of the just completed ionogram scaling are written/overwritten in the output file. TOPIST will remind the user if no profile inversion

was done before going to the next. If the scaling results are completely unsatisfactory, just click the box *UNDO*. This will restore the initial conditions, and the scaling can be started again.

Figures 13b and 14b show the results after manual scaling for Figures 13a and 14a. The agreements of the recalculated O, X and Z traces with the measured traces indicate very good scaling.

### **3.12 Testing of TOPIST**

The testing of TOPIST is based on about 800 topside ionograms, which were selected from the available ISIS-2 digital ionogram data files. This database includes ionograms

- From high, medium and low latitudes;
- For the time periods with low and high solar activities;
- With different trace features: different trace shapes; O and X traces cross at one, two or more frequencies; complete traces or data missing; different spread levels and different appearances of ground returns.

The tests on this database show that TOPIST can successfully auto-scale about 70% of the manually scalable ionograms. Scaling failures are the result of

- Wrong identification of resonance/cutoff frequencies; and/or
- Wrong separation of the O trace points from the X's.

These mistakes happen mostly for ionograms with severe spread. Since the success of the automatic scaling is very case dependent, testing must be repeated on the entire test database after any modification of the TOPIST algorithms. It should be stressed that the current database is established from the digital ISIS-2 ionograms.

## **4.0 Processing of ISIS Data**

This part of the project involved two tasks, both geared towards making topside sounder data available for ionospheric modeling activities. The first task was the processing of older Alouette and ISIS data sets of topside electron density profiles into a user-friendly and easily accessible form, and the second task was the processing of the digital ISIS ionograms into topside electron density profiles using the TOPIST software described in the previous sections.

### **4.1 Alouette and ISIS Satellites and their Orbit Characteristics.**

The Alouette 1, 2 and ISIS 1, 2 satellites were ionospheric observatories designed and operated jointly by the USA and Canada. The primary goal was a comprehensive investigation of the topside ionosphere using remote sensing and insitu instruments. The launch dates and orbit characteristics for the four satellites are listed in Table 1. Alouette 1 and 2 did not carry a tape recorder. Data could only be sent down when the spacecraft was in line of sight of telemetry stations. ISIS 1 and 2 included a tape recorder with a 1-hour capacity. Fortunately, a large number of ground stations were available for these topside sounder missions. The 24 primary stations are listed in Table 1 and their geographic location is indicated in Figure 15 illustrating the good global coverage provided.

NASA support of the ISIS project was terminated on October 1, 1979. Partial operations were continued by the Canadian project team until March 9, 1984 and were then resumed by the

**TABLE 1.** Orbit Characteristics of the Alouette/ISIS Satellites

Satellite	Launch Date	Height Range /km	Inclination/de gree
Alouette 1	1962-09-29	1000	80
Alouette 2	1965-11-29	500-3000	80
ISIS 1			
ISIS 2	1971-04-01	1400	88

**TABLE 2.** Primary Alouette/ISIS telemetry ground stations and the number of telemetry tapes that were included in the digitization effort.

Location	Station ID	Latitude	Longitude	Al-1	Al-2	ISIS-1	ISIS-2
Resolute Bay, Canada	RES	75	265			327 (76)	504 (73 79)
Tromsø, Norway	TRO.TRM	70	19			320	141 (73 76)
Sodankyla, Finland	SOD	67	27				63 (77 79)
Fairbanks, Alaska	ULA	65	212	1(62)		244 (73 79)	439 (73 79)
Winkfield, UK	WNK	51	359		2(66)	319	405 (73 79)
Ottawa, Canada	OTT	45	284			1187(69 83)	991 (73 83)
Kashima, Japan	KSH	36	141			103 (78 81)	879 (73 79)
Las Palmas Canary Island, Spain	CAN	28	345				106 (74 75)
Ahmedabad, India	AME	23	73				265 (73 77)
Ouagadougou, Burkina Faso	ODG	14	359			745 (73 79)	214 (73 75)
Kwajalein, Marshall Islands	KWA	9	168				140
Kourou, French Guyana	KRU	5	307				212 (74 77)
Quito, Ecuador	QUI	-1	281	1(62)	700	483 (69 72)	366 (73 79)
Brazzaville, Congo	BRZ.BZV	-4	15				34 (73 74)
Ascension Island, UK	ACN	-8	346				174 (75 77)
Lima, Peru	LIM	-12	283		11		
Johannesburg, South Africa	BUR.JOB	-26	28				192 (73 75)
Santiago, Chile	SNT.AGO	-33	298		428	209 (69)	240 (73 76)
Orroral, Australia	ORR	-36	149			66 (72 74)	232 (723 78)
Lauder, New Zealand	LAU	-45	170				604 (73 80)
Kerguelen Islands, France	KER	-49	70			98 (81 83)	464 (77 83)
Falkland Island, UK	SOL	-52	302		421		45 (72)
Terre Adelie, Antarctica	ADL	-67	140			54 (82 83)	738 (73 83)
Syowa Base, Antarctica	SYO	-69	40				241 (78 82)

\*For each of the four satellites the number of tapes is shown and in parentheses the years covered.

Japanese Radio Research Laboratories (Kashima ground station) from August 1984 to January 24, 1990.

A good summary of the Alouette and ISIS Program and its results can be found in a special issue of the Proceedings of the IEEE (Schmerling and Languille, 1969) and in two NSSDC reports by Jackson (1986, 1988).

The primary instrument was the topside sounder that was flown on all four satellites. The data accumulated by the Alouette and ISIS topside sounder instruments provide a unique global mapping of the topside ionosphere over more than a solar cycle.

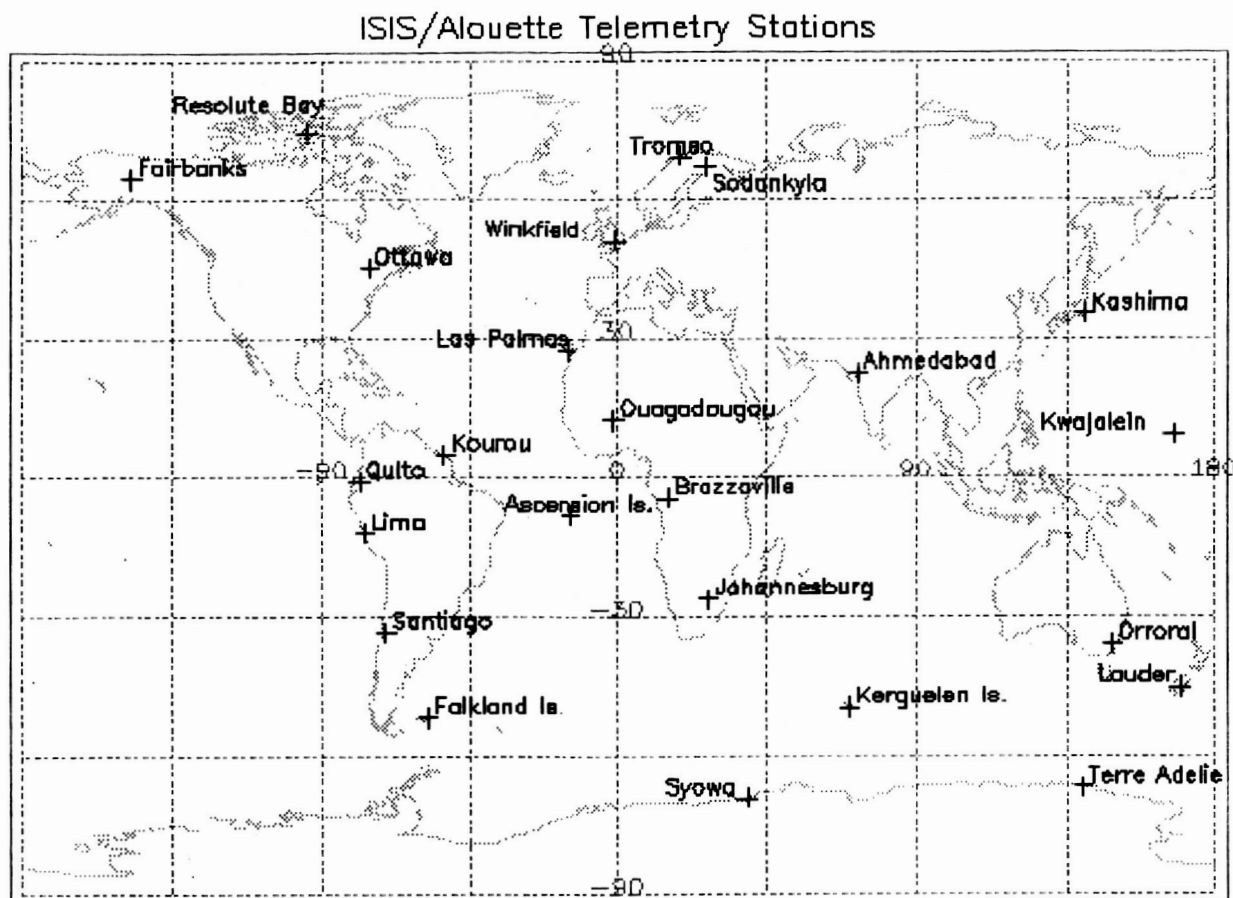


**Figure 15.** World map with location of Alouette/ISIS ground stations.

**4.1.1 Alouette 1** (Alouette is the French word for Lark) carried an ionospheric sounder, a VLF receiver, an energetic particle detector, and a cosmic noise experiment. Extended from the satellite shell were two dipole antennas (45.7- and 22.8-m long, respectively), which were shared by three of the experiments on the spacecraft. The satellite was spin-stabilized at about 1.4 rpm after antenna extension. After about 500 days, the spin slowed more than had been expected, to about 0.6 rpm when satellite spin-stabilization failed. It is believed that the satellite gradually progressed toward a gravity gradient stabilization with the longer antenna pointing earthward. Attitude information was deduced only from a single magnetometer and temperature measurements on the upper and lower heat shields. (Attitude determination could have been in error by as much as 10 deg.) Initially, data were recorded for about 6 h per day. In September 1972, spacecraft operations were terminated.

**4.1.2 Alouette 2** carried an ionospheric sounder, a VLF receiver, an energetic particle experiment, a cosmic noise experiment, and an electrostatic probe. The spacecraft used two long dipole antennas (73 m and 22.8 m, respectively) for the sounder, VLF, and cosmic noise experiment. The satellite was spin-stabilized at about 2.25 rpm after antenna deployment. End plates on the 73 m antenna corrected the rapid despin that had occurred on Alouette 1, and which was believed to result from thermal distortion of the antenna and from radiation pressure.

Initially data were recorded about 8 h per day. Degradation of the power supply system had, by June 1975, reduced the operating time to about 1/2 h per day. Routine operations were terminated in July 1975. The spacecraft was successfully reactivated on November 28 and 29, 1975, in order to obtain data on its 10th anniversary.

**4.1.3 *ISIS 1*** (International Satellite for Ionospheric Studies) carried a sweep- and fixed-frequency ionosonde, a VLF receiver, energetic and soft particle detectors, an ion mass spectrometer, an electrostatic probe, an electrostatic analyzer, a beacon transmitter, and a cosmic noise experiment. The sounder used two dipole antennas (73 and 18.7 m long). The satellite was spin-stabilized at about 2.9 rpm after antenna deployment. Some control was exercised over the spin rate and attitude by using magnetically induced torques to change the spin rate and to precess the spin axis. The satellite could be programmed to take recorded observations for four different time periods for each full recording period.

**4.1.4 *ISIS 2*** carried a sweep- and a fixed-frequency ionosonde, a VLF receiver, energetic and soft particle detectors, an ion mass spectrometer, an electrostatic probe, a retarding potential analyzer, a beacon transmitter, a cosmic noise experiment, and two photometers. Two long crossed-dipole antennas (73 and 18.7 m) were used for the sounding, VLF, and cosmic noise experiments. The spacecraft was spin-stabilized to about 2 rpm after antenna deployment. There were two basic orientation modes for the spacecraft, cartwheel and orbit-aligned. The spacecraft operated approximately the same length of time in each mode, remaining in one mode typically 3 to 5 months. The cartwheel mode with the axis perpendicular to the orbit plane was made available to provide ram and wake data for some experiments for each spin period, rather than for each orbit period. Attitude and spin information was obtained from a three-axis magnetometer and a sun sensor. Control of attitude and spin was possible by means of magnetic torquing.

## **4.2 Converting Existing NSSDC Data Sets to ASCII.**

A large amount of Alouette and ISIS topside sounder data are archived at NSSDC as original ionograms on microfilm (12,304 rolls off 35mm film and 17 rolls of 16mm film) and microfiche. A number of institutions worldwide were involved in efforts to obtain electron density profiles from the topside ionograms. Unfortunately, this required, at the time, a tedious and highly subjective manual scaling of the ionograms. The X- and O-traces were read from the ionograms and then fed into a computer and inverted to electron density profiles. Many of the data processing centers used the inversion algorithm (and program) developed by Jackson (1969). Because of the time required to manually scale the ionograms and because of the potential errors involved only a few percent of the hundred-thousands of ionograms were inverted to electron density profiles. Six of these electron density data sets were submitted to NSSDC in highly-compressed binary format on 9-track tapes. The data sets also include orbit parameters, solar and magnetic indices, the gyro frequency at the satellite height, and sometimes the F peak height and density and the electron content from satellite height down to the lowest point of reflection. We have decoded and converted these data into a common ASCII data format and have made these data available online on NSSDC's anonymous ftp site at [ftp://nssdcftp.gsfc.nasa.gov/spacecraft\\_data/](ftp://nssdcftp.gsfc.nasa.gov/spacecraft_data/) (go to ISIS or Alouette, then Topside Sounder, then CRC data set). The time period covered by these data sets and the number of profiles and the



total volume in Megabytes are listed in Table 3. Figure 16 shows that these data cover almost two solar cycles. Details about the individual data sets follow below.

**TABLE 3.** Characteristics of Alouette and ISIS data sets

Satellite	Time Period yyddd	Number of Profiles	Volume in MByte
Alouette 1a	62273 - 63082	15,706	6.7
Alouette 1b	62272 - 66089	43,614	12
Alouette 1c	62323 - 71350	26,452	5.8
Alouette 2	65349 - 72192	9,301	2.8
ISIS 1	69033 - 71087	38,953	8.2
ISIS 2	71098 - 79239	42,596	8.4

**4.2.1 Alouette 1 CRC Data Set 1.** This data set ('a' in Table 1; NSSDC-ID: 62-049A-01U) was prepared by the Communications Research Center in Ottawa, Canada, consisting of 15,706 electron density profiles from 1000 km down to the F peak. The original data were provided on 9-track, 1600-bpi, odd-parity, EBCDIC tape and were written on an MODCOMP-4 computer. The profiles were computed from digital values of frequency and virtual height that were scaled from ionograms. Profile data consist of electron density and real height values for each point scaled from the ionogram.

**4.2.2. Alouette 1 UCLA Data Set.** This data set ('b' in Table 1; NSSDC-ID: 62-049A-01P) was prepared at the University of California Los Angeles (UCLA) Department of Meteorology and consists of 43,596 electron density profiles of the ionosphere from 1000 km down to the F peak. The data were originally on a 7-track, 800-bpi, odd-parity, binary magnetic tape and were written on an IBM 360 computer. For many profiles the extrapolated maximum density and its real height are included. Profile data consist of density and real height values for each 25 km from 1000 km down to the lowest topside height from which reflections were observed. The electron density at the satellite altitude is also provided.

**4.2.3 Alouette 1 CRC Data Set 2.** This data set ('c' in Table 1; NSSDC-ID: 62-049A-01T) was provided by the Communications Research Center (CRC) in Ottawa, Canada and consists of 26,452 electron density profiles from 1000 km down to the F peak. The data were originally on 9-track, 1600-bpi, odd-parity, EBCDIC tape and were written on an MODCOMP-4 computer. The original data set provided a set of coefficients from which the heights could be calculated using the method described by Jackson (1969). Our NSSDC data set includes the calculated heights but not the original coefficients.

**4.2.4 Alouette 2 CRC Data Set.** This data set (NSSDC-ID: 65-098A-01O) was provided by the Communications Research Center (CRC) in Ottawa, Canada and consists of 9,301 electron density profiles from the satellite altitude (500-3000km) down to the F peak. The original data set was provided on an EBCDIC magnetic tape written on an IBM 360 computer. The electron density profiles were computed from digital values of frequency and virtual height, scaled from ionograms. The original data set provided a set of coefficients from which the heights could be calculated as explained in section 2.3.

**4.2.5 ISIS 1 CRC Data Set.** This data set (NSSDC-ID: 69-009A-01F) was prepared by the Communications Research Center (CRC) in Ottawa, Canada and consists of 38,953 electron density profiles from the satellite height (500-3500km) down to the F peak. The original data set was provided on binary magnetic tapes, written on an IBM 360 computer. Heights were provided in the same way as for the data sets described in sections 2.4 and 2.5.

**4.2.5 ISIS 2 CRC Data Set.** This data set (NSSDC-ID: 71-024A-01F) was prepared by the Communications Research Center (CRC) in Ottawa, Canada and consists of 42,596 electron density profiles from the satellite height (500-3500km) down to the F peak. The original data set was provided on binary magnetic tapes, written on an IBM 360 computer. Heights were provided in the same way as for the data sets described in sections 2.4 and 2.5.

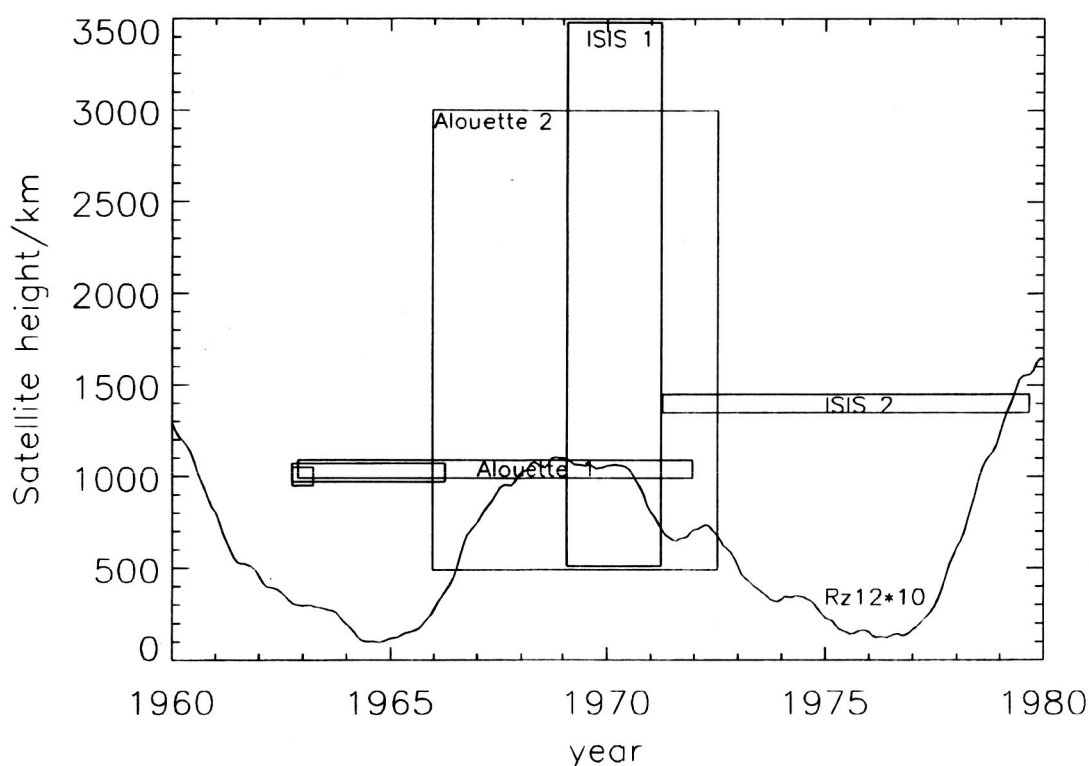


Fig. 16. Time periods of data sets in relation to solar cycle as given by the 12-month running mean of sunspot number (Rz12).

### 4.3 TOPIST Processing of Digital ISIS-2 Ionograms.

The TOPIST software as described in Section 2 was used to process the digital topside ionograms that have recently become available in the framework of a NASA-funded data rescue and restoration effort (see <http://nssdc.gsfc.nasa.gov/space/isis/isis-status.html>). Of the close to one million ionograms recorded by the Alouette/ISIS satellites, several tens of percent are stored on more than 12,000 rolls of 35 mm microfilm at the National Space Science Data Center (NSSDC) and only a few percent of the ionograms were processed into electron density profiles, e.g., the 167,414 profiles described in Section 4.2. The full Alouette/ISIS data were stored on



about 100,000 7-track telemetry tapes in the Canadian Public Archives (CPA). In the early 1990s the CPA indicated its intent to discard these tapes because of storage space and cost limitations. A data rescue effort led by G. James (CRC) and R. Benson (GSFC) was able to save ~18,000 of these tapes, specifically selected for good coverage in terms of solar cycle, season and global location, and to ship them to the GSFC (one of the few sites that still had an operating tape drive that could read 7-track analog tapes) for processing and analysis. The rest of the telemetry tapes were discarded, and the information contained on them is now lost.

Working with the old telemetry tapes and often insufficient documentation the digitization team had to overcome a number of hurdles in working its way through processing the saved telemetry tapes. TOPIST-processing of the digital ionograms was done in close coordination with the digitization group and has led to improvements of the digitization as well as the TOPIST software. For example, the identification of frequency markers, which are embedded in the receiver video output, was improved in the digitization software in going from ISIS-2 (which was done first) to ISIS-1.

TOPIST processing has focused on the ISIS-2 digital data, since digitization for these data was completed during the project time period (including several no-cost extensions). The results of this effort are as follows (an example page of processing statistics by year and station is listed in APPENDIX C):

Total number of available ISIS-2 digital ionograms:	306,403
Number of ionograms that TOPIST could read	275,215
Number of ionograms that were successfully scaled and inverted	145,025

The majority of the TOPIST processing failures are in fact not due to limitations of the TOPIST scaling but rather due to insufficient information provided in the digital ionogram files. For example, for OTTAWA 1973 we find:

Total number of files	3229
Total number of failures	1105
Failure reasons:	
Invalid transmitter code found	208
Negative frequency markers found	429
Not usable - starting swept frequency > 0.1 Mhz	304
Not usable - non-monotonic frequency markers found	67
Not usable - the file is not complete	91
Data error found or format inconsistency	2
Total	1105

A number of these problems could be overcome with the more recent identification scheme for frequency markers that was used for the ISIS-1 digitization. It looks at the frequency differences rather than absolute values to identify the standard frequency markers. If this same algorithm could be implemented in TOPIST as a pre-processing step it might be possible to produce electron density profiles for many more cases that are now thrown out for the reasons listed above.

But even with the current limitations and working only with ISIS-2 our project has produced a new data set of 145,025 electron density profiles for topside modeling, thereby doubling the amount of profiles previously available from Alouette and ISIS. With the indicated changes to the TOPIST software and with processing of the ISIS-1 and Alouette digital ionograms this database will increase even further.

## 5.0 References

- Belehaki, A., P. Marinov, I. Kutiev, N. Jakowski, and S. Stankov, Comparison of the topside ionosphere scale height determined by topside sounders model and bottomside Digisonde profiles, submitted to Advances in Space Research, 2005.
- Bilitza, D., International Reference Ionosphere 1990, *NSSDC Report 90-22* National Space Science Data Center, Greenbelt, Maryland, USA, 1990.
- Bilitza, D., International Reference Ionosphere 2000, *Radio Sci.*, 36, 2, 261-275, 2001.
- Bilitza, D., A correction for the IRI topside electron density model based on Alouette/ISIS topside sounder data, *Adv. Space Res.* 33, #6, 838-843, 2004.
- Bent, R. B., S. K. Llewellyn, and M. K. Walloch, Description and Evaluation of the Bent Ionospheric Model," Space & Missile Systems Organization, Report SAMSO TR-72-239, Los Angeles, California, 1972.
- Budden, K.G., The propagation of radio waves, Cambridge University Press, 1985.
- CCIR, Comité Consultatif International des Radiocommunications, Report 340-1, 340-6, ISBN 92-61-04417-4, Genève, Switzerland, 1966.
- Galkin, I.A., B.W. Reinisch, G.A. Osokov, E.G. Zazobina, and S.P. Neshyba, Feedback neural networks for ARTIST ionogram processing, *Radio Sci.*, 31, 5, 1119-1128, 1996.
- Hagg, E.L., E.J. Hewens, and G.L. Nelms, The interpretation of topside ionograms, *Proc. IEEE*, 57, 949-960, 1969.
- Huang, X. and B.W. Reinisch, Automatic Calculation of Electron Density Profiles from Digital Ionograms. 2. True Height Inversion of Topside Ionograms with the Profile-Fitting Method, *Radio Sci.*, 17, 4, 837-844, July-August 1982
- Jackson, J.E., The reduction of topside ionograms to electron-density profiles, *Proc. IEEE*, 57(6), 960-976, 1969.
- Jackson, J.E., E.R. Schmerling, and J.H. Whittecker, Mini-review on topside sounding, *IEE Trans. Antennas Propagation*, AP-28, 284-288, 1980.
- Jackson, J.E., Alouette ISIS Program Summary, National Space Science Data Center, Report 86-09, Greenbelt, Maryland, August 1986.
- Jackson, J.E., Results from Alouette 1, Explorer 20, Alouette 2, and Explorer 3, National Space Science Data Center, Report 88-10, Greenbelt, Maryland, July 1988.
- Kutiev, I., P. Marinov, S. Watanabe, Model of topside ionosphere scale height based on topside sounder data, submitted to Advances in Space Research, 2005
- Marinov, P., I. Kutiev, and S. Watanabe, Empirical model of  $O^+ - H^+$  transition height based on topside sounder data, *Adv. Space Res.* 34, #9, 2021-2025, 2004.
- Muldrew, D.B., Topside-sounder resonances, *Proc. IEEE*, 57, 1089-1096, 1969.
- Muldrew, D.B., Electron resonances observed with topside sounders, *Radio Sci.*, 7, 779-789, 1972.

- Reinisch, B.W. and X. Huang, Automatic Calculation of Electron Density Profiles from Digital Ionograms, 1, Automatic 0 and X Trace Identification for Topside Ionograms, *Radio Sci.*, 17, 2, 421-434, 1982.
- Reinisch, B.W. and X. Huang, Automatic Calculation of Electron Density Profiles from Digital Ionograms, 3, Processing of Bottomside Ionograms, *Radio Sci.*, 18, 3, 477-492, 1983.
- Reinisch, B.W., Modern Ionosondes, in *Modern Ionospheric Science*, (Eds. H. Kohl, R. Rüster, and K. Schlegel), European Geophysical Society, 37191 Katlenburg-Lindau, ProduServ GmbH Verlagsserie, Berlin, Germany, 440-458, 1996.
- Reinisch, B.W., SAO (Standard ADEP Output) format for ionogram scaled data archiving, *INAG Bulletin No. 62*, WDC-A for STP, Boulder, CO, 47-58, 1998.
- Rush, C., M. Fox, D. Bilitza, K. Davies, L. McNamara, F. Stewart, and M. PoKempner, Ionospheric Mapping – An Update of foF2 Coefficients, *Telecommunication Journal*, 56, pp. 179-182, 1989.
- Schmerling, E.R., and R.C. Languille, Special Issue on Topside Sounding and the Ionosphere, *Proceedings of the IEEE*, 57, #6, 859-1240, 1969.
- Titheridge, J.E. and R.J. Lobb, A least square polynomial analysis and its application to topside ionograms, *Radio Sci.*, 12(3), 451-459, 1977.
- Coïsson, P., S.M. Radicella, R. Leitinger, B. Nava, Topside electron density in IRI and NeQuick, submitted to *Advances in Space Research*, 2005.
- Webb, P. A. and R. F. Benson, Altitude variations of middle-latitude topside ionospheric electron-density profiles, submitted to *Advances in Space Research*, 2005.

## **APPENDIX A: Instructions for TOPIST Operation**

### **1. HARDWARE AND OPERATING SYSTEM**

The Program TOPIST.exe is used to process the digital topside ionograms from the sounders on the satellites Alouette and ISIS. The Program is only executable in a PC with at least 128 Mbytes RAM, and with an operating system MS Windows 98/2000 or MS Windows NT.

### **2. INSTALLATION**

The Program TOPIST.exe and the associated data files for the CCIR/URSI coefficients and sunspot numbers should be loaded together in one subdirectory.

### **3. PROGRAM INVOKING**

The command line to invoke the program specifies the required parameters for processing topside ionograms, consisting of at most 8 items:

**Item\_1 Item\_2 Item\_3 Item\_4 Item\_5 Item\_6 Item\_7 Item\_8**

One space separates one item from another and there should be no spaces in any item inside itself. If there are more than 8 items, the items after the 8th will be disregarded. The syntax for each item is as described below.

- **Item\_1=TOPIST\_path:TOPIST**  
If TOPIST is loaded at the current drive and subdirectory, "TOPIST\_path:" can be omitted.
- **Item\_2=An integer**, specifying the input data type: 1 denotes binary coded format and 2 CDF format. The current TOPIST accepts only binary coded ionogram data files.
- **Item\_3=An integer**, specifying the scaling mode: 1 for automatic scaling, 2 for manual scaling, and 3 for automatic scaling first and then manual scaling.
- **Item\_4=An integer**, specifying whether raw ionograms are displayed on the screen: 1 for display, and 0 for no display.
- **Item\_5=An integer**, showing if noise-filtered ionograms are displayed on the screen: 1 for display, and 0 for no display.
- **Item\_6=An integer**, showing if message widows are displayed on the screen: 1 for display, and 0 for no display.
- **Item\_7=Input\_path:Input\_file\_name.**  
The part of "Input\_path" includes the DRIVE and the full path. The part of "Input\_file\_name" may be the name of any one ionogram data file. If "\*. \*" appears in this part, the first "\*" denotes any file name and the second "\*" denotes any extension name of the file, and so it means all the files in the specified path are included.
- **Item\_8=Output\_path:Output\_file\_name.**  
In the part of "Output\_path" includes the DRIVE and the full path. If the input file is one ionogram data file, any output file name specified with a character

string is acceptable. If the Input\_file\_name is specified as \*.\* , the Output\_file\_name should be specified as

**A\*B.D or A\*B\*C.D**

Here A, B and C denote character strings and D the extension name. The first \* is taken from the input file name and the second \* from the extension name of the input file. The string A, B or/and C may have zero length (but not all of them). The whole length of the output file name including the extension name should be no longer than 256.

For example, the following names are all legal:

**\*.TOP  
\*.\*.TOP  
TOPIST\*.TOP  
TOPIST\*.\*.TOP  
\*NASA.TOP  
\*NASA\*.TOP  
TOPIST\*NASA.TOP  
TOPIST\*NASA\*.TOP  
TOPIST\*NASA\*\_2001.TOP**

Corresponding to the input file

**80185143832KSH\_AVG\_ISIS2TOPS\_24S.OS2BIN**

the output file name will be one of the following:

**80185143832KSH\_AVG\_ISIS2TOPS\_24S.TOP  
80185143832KSH\_AVG\_ISIS2TOPS\_24S.OS2BIN.TOP  
TOPIST80185143832KSH\_AVG\_ISIS2TOPS\_24S.TOP  
TOPIST80185143832KSH\_AVG\_ISIS2TOPS\_24S.OS2BIN.TOP  
80185143832KSH\_AVG\_ISIS2TOPS\_24SNASA.TOP  
80185143832KSH\_AVG\_ISIS2TOPS\_24SNASAOS2BIN.TOP  
TOPIST80185143832KSH\_AVG\_ISIS2TOPS\_24SNASA.TOP  
TOPIST80185143832KSH\_AVG\_ISIS2TOPS\_24SNASAOS2BIN.TOP  
TOPIST80185143832KSH\_AVG\_ISIS2TOPS\_24SNASAOS2BIN\_2001.TOP**

One can invoke the program with only the first one item, or the first two items, or the first three items, etc. When the parameters specified with the command line are not complete, TOPIST will ask for specifying other parameters. If there are any illegal entries in any item, the error message will be shown in a message window on the screen and TOPIST will terminate execution.

#### **4. LOG FILES**

Two log files are always created in the same location as the output files after TOPIST completes processing. The first one records the file names with which the files were successfully processed and the second records the file names with which some data errors or execution errors were found in the data files.

If TOPIST finds not enough space to create the output files, TOPIST will terminate processing and give a message in a window.

#### **5. AUTOMATIC SCALING**

STEP 1: Load ionogram data files in a subdirectory. The limitation for the number of files depends on the disk size of the computer.

STEP 2: Create a subdirectory for output file storage. There should be enough space for it. Otherwise, TOPIST will terminate processing once it finds no more space to create output files.

STEP 3: Use a command to invoke TOPIST (See Section 3)

**TOPIST 1 1 0 0 0 INPUT\_FULL\_PATH:\*. \* OUTPUT\_FULL\_PATH:A\*B\*C.D**

Then TOPIST will process all the data files and nothing is displayed on the screen.

If one needs the processing message shown on the screen, the following command can be used:

**TOPIST 1 1 0 0 1 INPUT\_FULL\_PATH:\*. \* OUTPUT\_FULL\_PATH:A\*B\*C.E**

If one invokes the program in a subdirectory other than where the Program TOPIST is loaded, the full path should be added to the above command for invoking.

#### **6. MANUAL SCALING/EDITTING**

STEP 1: Load ionogram data files in a subdirectory, and load the corresponding output files if available from previous automatic scaling in another subdirectory.

STEP 2: To invoke the program use the command

**[TOPIST\_FULL\_PATH:]TOPIST**

Then the ionogram will be processed one by one.

It is convenient to create an icon to show the shortcut to invoke the program. When the icon is clicked TOPIST is invoked.

## APPENDIX B: An Example of the TOPIST Output Files

```

*(01) IONOGRAM DATA FILE NAME: 80185143832KSH_AVG_ISIS2TOPS_24S.OS2BIN
*(02) SATELLITE (NAME, HEIGHT[km], GYRO-FREQUENCY[MHz],DIP-ANGLE[DEGREES]):
ISIS-2 1410.268 0.811 66.000
*(03) TIME (UT YYYY DOY MM DD HH MM SS; LMT HH MM; GMLT HH MM):
1980 185 07 03 14 38 32 00 40 00 08
*(04) LOCATION[DEGREES] (GG-LATITUDE, LONGITUDE; GM-LATITUDE, LONGITUDE; SHELL):
54.270 150.461 44.707 -148.519 2.567
*(05) SOLAR-TERRESTRIAL PARAMETERS (SUNSPOT NUMBER AND ZENITH[DEGREES]):
152.800 103.000
*(06) SCALING STATUS (TOOL, STATUS-CODE[1,2,3], REMARK):
TOPIST_2000.12 1: AUTO-SCALED
*(07) SCALING CONCLUSION (CONCLUSION-CODE, REMARK):
0 SUCCESSFUL INVERSION
*(08) SCALED: foF2[MHz], hmF2[km], AND MODELED: foF2[MHz], hmF2[km]
8.080 352.722 7.392 364.059
*(09) RESONANCE & CUTOFF FREQUENCIES[MHz] (FZS,FNS,FTS,FXS,CYCLOTRON HARMONICS):
0.740 1.072 1.345 1.553
0.813 1.626 2.439 0.000 0.000 0.000 0.000 0.000 0.000 0.000
*(10) FREQUENCY TABLE (INDICES OF SCAN STARTING AND ENDING, FREQUENCY[MHz]):
147 640
0.100 0.108 0.116 0.117 0.124 0.132 0.140 0.148 0.156 0.164
0.171 0.179 0.187 0.195 0.203 0.211 0.219 0.227 0.234 0.242
0.250 0.258 0.266 0.273 0.281 0.289 0.297 0.305 0.312 0.320
0.328 0.336 0.344 0.351 0.359 0.367 0.375 0.383 0.390 0.398
0.406 0.414 0.422 0.429 0.437 0.445 0.453 0.461 0.469 0.476
0.484 0.492 0.500 0.508 0.516 0.524 0.532 0.540 0.548 0.556
0.564 0.572 0.581 0.589 0.597 0.605 0.613 0.621 0.629 0.637
0.645 0.653 0.661 0.669 0.678 0.686 0.694 0.702 0.710 0.718
0.726 0.734 0.742 0.750 0.758 0.766 0.774 0.781 0.789 0.797
0.805 0.813 0.820 0.828 0.836 0.844 0.852 0.859 0.867 0.875
0.883 0.891 0.898 0.906 0.914 0.922 0.930 0.937 0.945 0.953
0.961 0.969 0.976 0.984 0.992 1.000 1.008 1.016 1.024 1.032
1.040 1.048 1.056 1.064 1.072 1.081 1.089 1.097 1.105 1.113
1.121 1.129 1.137 1.145 1.153 1.161 1.169 1.178 1.186 1.194
1.202 1.210 1.218 1.226 1.234 1.242 1.250 1.258 1.266 1.274
1.281 1.289 1.297 1.305 1.313 1.320 1.328 1.336 1.344 1.352
1.359 1.367 1.375 1.383 1.391 1.398 1.406 1.414 1.422 1.430
1.437 1.445 1.453 1.461 1.469 1.476 1.484 1.492 1.500 1.508
1.516 1.524 1.532 1.540 1.548 1.556 1.564 1.572 1.581 1.589
1.597 1.605 1.613 1.621 1.629 1.637 1.645 1.653 1.661 1.669
1.678 1.686 1.694 1.702 1.710 1.718 1.726 1.734 1.742 1.750
1.758 1.766 1.774 1.782 1.790 1.798 1.806 1.814 1.822 1.830
1.838 1.846 1.853 1.861 1.869 1.877 1.885 1.893 1.900 1.908
1.916 1.924 1.931 1.939 1.947 1.954 1.962 1.970 1.977 1.985
1.992 2.000 2.024 2.047 2.071 2.095 2.118 2.142 2.165 2.189
2.212 2.236 2.259 2.283 2.306 2.329 2.353 2.376 2.399 2.423
2.446 2.469 2.493 2.516 2.539 2.562 2.585 2.609 2.632 2.655
2.678 2.701 2.724 2.747 2.770 2.793 2.816 2.839 2.862 2.885
2.908 2.931 2.954 2.977 3.000 3.023 3.046 3.069 3.092 3.114
3.137 3.160 3.183 3.206 3.229 3.251 3.274 3.297 3.320 3.342
3.365 3.388 3.411 3.433 3.456 3.479 3.501 3.524 3.547 3.570
3.592 3.615 3.638 3.660 3.683 3.706 3.728 3.751 3.774 3.796
3.819 3.842 3.864 3.887 3.909 3.932 3.955 3.977 4.000 4.023
4.045 4.068 4.091 4.113 4.136 4.158 4.181 4.204 4.226 4.249
4.272 4.294 4.317 4.340 4.362 4.385 4.408 4.430 4.453 4.476
4.499 4.521 4.544 4.567 4.589 4.612 4.635 4.658 4.680 4.703
4.726 4.749 4.771 4.794 4.817 4.840 4.863 4.886 4.908 4.931
4.954 4.977 5.000 5.045 5.090 5.134 5.179 5.223 5.267 5.311
5.355 5.399 5.442 5.486 5.529 5.573 5.616 5.659 5.702 5.745
5.787 5.830 5.873 5.915 5.958 6.000 6.042 6.084 6.127 6.169
6.211 6.252 6.294 6.336 6.378 6.420 6.461 6.503 6.544 6.586
6.627 6.669 6.710 6.752 6.793 6.835 6.876 6.917 6.959 7.000
7.042 7.084 7.126 7.168 7.210 7.252 7.293 7.335 7.377 7.419
7.461 7.502 7.544 7.586 7.627 7.669 7.711 7.752 7.794 7.835
7.876 7.918 7.959 8.000 8.040 8.080 8.120 8.160 8.200 8.239
8.279 8.319 8.359 8.398 8.438 8.478 8.518 8.558 8.597 8.637
8.677 8.717 8.757 8.798 8.838 8.878 8.919 8.959 9.000 9.041
9.082 9.123 9.164 9.205 9.247 9.289 9.331 9.373 9.415 9.458
9.500 9.543 9.586 9.630 9.673 9.717 9.761 9.806 9.850 9.895
9.941 9.986 10.032 10.078
*(11) TRUE HEIGHT (INDICES OF STARTING AND ENDING FREQUENCIES, HEIGHT[km]):
271 592
1410.2681397.7961387.0711376.6671366.5661356.7531347.2131337.9321328.8971320.095
1311.5151303.1471294.9791286.0181278.2451270.6461263.2111255.9331248.8061241.823
1234.9781228.2641221.6771215.2111208.8621202.6251197.2551191.2161185.2771179.434
1173.6851168.7281163.1441157.6451152.2271146.8881142.2791137.0821131.9561126.901
1121.9141117.6041112.7401107.9381103.1971098.5171094.4691089.8961085.3791080.917

```



1076.5081072.6931068.3801064.1171059.9041055.7391051.6201047.5481043.5211039.539  
 1035.6011031.7051027.8521024.0411019.8011016.0761012.3891008.7421005.1331001.562  
 998.028 994.530 991.069 987.643 984.253 980.896 977.162 973.877 970.626 967.408  
 964.222 961.068 957.946 954.854 951.794 948.763 945.763 942.792 939.850 936.937  
 934.052 931.196 928.367 925.566 922.792 920.045 917.324 914.630 912.293 909.647  
 907.026 904.430 901.858 899.312 897.103 894.601 892.122 889.667 887.537 885.125  
 882.735 880.662 878.314 875.987 873.969 871.683 869.699 867.451 860.831 854.654  
 848.376 842.265 836.558 830.753 825.330 819.812 814.653 809.399 804.486 799.479  
 794.792 790.211 785.538 781.160 776.876 772.502 768.399 764.381 760.273 756.417  
 752.635 748.925 745.285 741.558 738.052 734.609 731.225 727.899 724.629 721.413  
 718.249 715.134 712.068 709.049 706.075 703.144 700.256 697.408 694.600 691.830  
 689.097 686.400 683.737 681.109 678.513 676.059 673.524 671.020 668.544 666.097  
 663.678 661.389 659.021 656.680 654.363 652.170 649.901 647.655 645.432 643.327  
 641.147 638.989 636.945 634.828 632.731 630.654 628.686 626.647 624.627 622.712  
 620.729 618.763 616.900 614.969 613.055 611.241 609.360 607.496 605.729 603.897  
 602.159 600.358 598.573 596.879 595.123 593.383 591.732 590.020 588.322 586.712  
 585.042 583.458 581.816 580.187 578.641 577.038 575.448 573.940 572.375 570.823  
 569.350 567.822 566.306 564.867 563.374 561.893 560.424 559.028 557.580 556.143  
 554.779 553.363 551.957 550.561 549.236 547.860 546.493 545.136 543.847 542.508  
 541.178 539.856 538.543 537.239 535.999 534.710 533.429 532.156 530.890 528.433  
 526.002 523.650 521.266 518.956 516.665 514.391 512.133 509.891 507.711 505.493  
 503.335 501.136 498.994 496.857 494.725 492.596 490.519 488.392 486.265 484.185  
 482.053 479.967 477.875 475.777 473.622 471.508 469.386 467.304 465.161 463.006  
 460.838 458.658 456.515 454.306 452.135 449.895 447.693 445.421 443.186 440.880  
 438.611 436.270 433.966 431.646 429.251 426.895 424.464 422.015 419.549 417.065  
 414.564 412.047 409.574 407.025 404.461 401.882 399.289 396.745 394.125 391.491  
 388.906 386.244 383.565 380.930 378.206 375.514 372.774 369.892 366.956 363.790  
 360.190 352.721

\*(12) PROFILE PARAMETERS (fs[MHz],fm[MHz],RM[km],A(1),...,A(8)[km]):

1.072 8.080 1057.546  
 -554.335 -389.859 -62.691 -50.046 11.399 -12.550 5.124 -4.588

\*(13) PROFILE QUALITY(1-3: 3=BEST), FREQUENCY RANGE[MHz] WITH HIGHER CONFIDENCE:

3 1.072 8.080

\*(14) O-TRACE (STARTING AND ENDING FREQUENCY INDICES, SPREAD[km], RANGE[km]):

346 510 11.250  
 922.500 922.500 922.500 922.500 922.500 922.500 933.750 937.500 937.500 937.500  
 943.128 945.824 948.520 951.215 953.911 956.606 959.302 961.998 964.693 967.389  
 970.085 972.780 975.476 977.834 980.530 983.226 985.921 988.617 991.313 993.671  
 996.367 999.0621001.7581004.1171006.8121009.5081011.8671014.5621017.2581019.617  
 1023.750 0.000 0.000 952.500 967.500 967.500 967.500 967.500 967.500 967.500  
 967.500 967.500 967.500 982.500 982.500 982.500 982.500 982.500 982.500 982.500  
 982.500 982.500 982.500 993.750 997.500 997.500 997.500 997.500 997.500 997.500  
 997.500 997.500 997.500 997.5001005.0001012.5001012.5001012.5001012.5001012.500  
 1012.5001012.5001012.5001012.500 0.000 0.0001012.5001012.5001020.0001027.500  
 1027.500 0.0001027.5001027.5001027.5001027.500 0.0001027.500 0.000 0.000  
 1027.5001027.5001027.500 0.000 0.000 0.000 0.0001042.5001042.5001042.500  
 1042.5001042.5001042.5001042.5001042.5001042.5001042.5001042.5001042.5001042.500  
 1042.5001057.5001057.5001053.7501057.5001057.5001057.5001057.500 0.000 0.000  
 1057.5001057.5001057.5001057.500 0.000 0.000 0.000 0.000 0.000 0.000  
 0.000 0.0001072.5001072.5001072.5001072.5001072.5001072.500 0.0001102.500  
 1102.5001102.5001102.500 0.0001102.5001087.500 0.000 0.000 0.000 0.000  
 1087.5001087.5001087.5001083.7501087.500

\*(15) X-TRACE (STARTING AND ENDING FREQUENCY INDICES, SPREAD[km], RANGE[km]):

346 607 18.750  
 757.500 772.500 787.500 787.500 810.000 813.750 817.500 847.500 847.500 855.000  
 844.229 850.696 857.162 863.629 870.096 876.563 883.029 889.496 895.963 902.430  
 908.896 915.363 921.830 927.488 933.955 940.422 946.888 953.355 959.822 965.480  
 971.947 978.414 984.880 990.539 997.0061003.4721009.1311015.5971022.0641027.723  
 1023.750 0.000 0.0001042.5001042.5001042.5001057.500 0.000 0.0001057.500  
 1072.5001087.5001087.5001087.5001102.5001102.5001102.5001072.5001072.5001072.500  
 1087.5001087.5001087.5001083.7501087.5001087.5001087.5001095.0001095.0001087.500  
 1087.5001087.5001087.5001087.5001087.500 0.0001087.5001087.5001087.5001087.500  
 1102.5001102.5001098.7501072.5001072.500 0.0001087.5001087.5001095.0001087.500  
 1087.500 0.0001087.5001095.0001087.5001087.500 0.0001087.500 0.000 0.000  
 1087.5001102.5001102.500 0.000 0.000 0.000 0.000 0.000 0.0001087.500  
 0.0001087.5001102.5001098.7501102.5001098.7501102.5001102.5001098.7501102.500  
 1102.5001102.5001102.5001098.7501102.5001102.5001102.5001102.500 0.000 0.000  
 1098.750 0.000 0.000 0.000 0.000 0.000 0.000 0.000 0.000 0.000  
 0.000 0.0001102.5001102.5001102.5001102.500 0.000 0.000 0.000 0.000  
 0.000 0.000 0.000 0.000 0.000 0.000 0.000 0.000 0.000 0.000  
 0.0001117.500 0.000 0.0001087.500 0.000 0.000 0.0001102.5001087.500  
 0.000 0.000 0.000 0.0001102.5001102.5001102.5001102.500110.0001128.750  
 1132.5001117.5001117.5001117.5001117.5001132.5001128.7501132.5001132.5001132.500  
 1132.5001132.5001132.5001132.5001132.500 0.000 0.0001147.5001147.5001147.500  
 1147.5001147.5001147.5001147.5001162.5001158.7501162.5001162.5001162.5001162.500  
 1162.5001162.5001177.5001177.5001177.5001177.5001177.5001185.0001177.500 0.000  
 0.0001207.5001207.5001215.0001222.5001192.5001192.5001192.5001237.5001207.500  
 1207.5001207.5001207.5001207.5001207.5001222.5001222.5001222.5001230.0001233.750  
 1237.5001260.0001263.750 0.000 0.0001275.0001278.7501282.5001290.0001293.750  
 0.0001301.2501305.0001308.7501316.2501320.000 0.0001327.5001335.0001338.750



### APPENDIX C: Example of Processing Statistics by Year and Station

STA ID	YR	FILENAME	TOPIST	FAIL	TOTAL	%
ACN_2_1975		TOPIST20020527225143_failure.LOG	336	156	492	68.29
ACN_2_1976		TOPIST20020528233357_failure.LOG	1159	195	1354	85.60
ACN_2_1977		TOPIST20020529195718_failure.LOG	159	83	242	65.70
ACN_2_1978		TOPIST20020529201132_failure.LOG	91	59	150	60.67
ADL_2_1973		TOPIST20020520133526_failure.LOG	705	3147	3852	18.30
ADL_2_1974		TOPIST20020520152428_failure.LOG	310	311	621	49.92
ADL_2_1974		TOPIST20020520163901_failure.LOG	10	6	16	62.50
ADL_2_1974		TOPIST20020520164145_failure.LOG	12	3	15	80.00
ADL_2_1974		TOPIST20020520164417_failure.LOG	171	97	268	63.81
ADL_2_1974		TOPIST20020520180225_failure.LOG	386	1351	1737	22.22
ADL_2_1975		TOPIST20020520215411_failure.LOG	763	1779	2542	30.02
ADL_2_1975		TOPIST20020520225458_failure.LOG	109	230	339	32.15
ADL_2_1976		TOPIST20020520230631_failure.LOG	81	261	342	23.68
ADL_2_1976		TOPIST20020520231654_failure.LOG	30	111	141	21.28
ADL_2_1976		TOPIST20020521105037_failure.LOG	455	2069	2524	18.03
ADL_2_1976		TOPIST20020521115620_failure.LOG	200	396	596	33.56
ADL_2_1976		TOPIST20020521134319_failure.LOG	40	19	59	67.80
ADL_2_1977		TOPIST20020521140308_failure.LOG	281	2279	2560	10.98
ADL_2_1978		TOPIST20020521151514_failure.LOG	161	899	1060	15.19
ADL_2_1978		TOPIST20020521160206_failure.LOG	197	545	742	26.55
ADL_2_1979		TOPIST20020521165142_failure.LOG	294	998	1292	22.76
ADL_2_1979		TOPIST20020521173054_failure.LOG	153	546	699	21.89
ADL_2_1979		TOPIST20020521182605_failure.LOG	173	246	419	41.29
ADL_2_1979		TOPIST20020521202137_failure.LOG	179	820	999	17.92
ADL_2_1980		TOPIST20020521212447_failure.LOG	370	1561	1931	19.16
ADL_2_1981		TOPIST20020521222101_failure.LOG	24	215	239	10.04
ADL_2_1981		TOPIST20020522110312_failure.LOG	383	1807	2190	17.49
ADL_2_1981		TOPIST20020522133448_failure.LOG	1	0	1	100.00
ADL_2_1981		TOPIST20020522133644_failure.LOG	4	37	41	9.76
AME_2_1973		TOPIST20020523102645_failure.LOG	798	4184	4982	16.02

AME_2_1973	TOPIST20020523145050_failure.LOG	73	610	683	10.69
AME_2_1974	TOPIST20020523155922_failure.LOG	693	3885	4578	15.14
AME_2_1975	TOPIST20020523202325_failure.LOG	259	787	1046	24.76
AME_2_1975	TOPIST20020523205651_failure.LOG	551	1556	2107	26.15
AME_2_1975	TOPIST20020524111515_failure.LOG	61	365	426	14.32
AME_2_1976	TOPIST20020524122515_failure.LOG	185	1112	1297	14.26
AME_2_1976	TOPIST20020524130527_failure.LOG	55	297	352	15.63
AME_2_1977	TOPIST20020524140620_failure.LOG	367	1837	2204	16.65
BRZ_2_1972	TOPIST20020527003953_failure.LOG	21	28	49	42.86
BRZ_2_1973	TOPIST20020527004304_failure.LOG	970	1767	2737	35.44
BRZ_2_1974	TOPIST20020527213809_failure.LOG	318	163	481	66.11
BRZ_2_1975	TOPIST20020527220712_failure.LOG	27	2	29	93.10
BUR_2_1972	TOPIST20020524153122_failure.LOG	38	3	41	92.68
BUR_2_1973	TOPIST20020524165407_failure.LOG	1184	197	1381	85.73
BUR_2_1974	TOPIST20020526140029_failure.LOG	35	50	85	41.18
BUR_2_1975	TOPIST20020526140246_failure.LOG	507	404	911	55.65
CNA_2_1974	TOPIST20020529204659_failure.LOG	974	278	1252	77.80
CNA_2_1974	TOPIST20020530224856_success.LOG	1	278	1	100.00
CNA_2_1975	TOPIST20020530235922_failure.LOG	1619	386	2005	80.75
KER_2_1977	\$TOPIST20020109174347_failure.LOG	10	1579	1589	0.63
KER_2_1978	\$TOPIST20020109175429_failure.LOG	7	985	992	0.71
KER_2_1979	\$TOPIST20020109211853_failure.LOG	7	793	800	0.88
KER_2_1980	\$TOPIST20020109220013_failure.LOG	19	1182	1201	1.58
KER_2_1981	TOPIST20020508123458_failure.LOG	24	945	969	2.48
KER_2_1982	TOPIST20020508124006_failure.LOG	14	1010	1024	1.37
ker_2_1983	TOPIST20020508124552_failure.LOG	3	478	481	0.62
KER_2_1984	TOPIST20020508124838_failure.LOG	3	154	157	1.91
KRU_2_1973	TOPIST20020619001945_failure.LOG	33	64	97	34.02

#### **APPENDIX D: Papers presented (speaker underlined):**

X. Huang, B. Reinisch, D. Bilitza, and R. Benson, New Data Source for Studying and Modelling the Topside Ionosphere, European Geophysical Society meeting, Nice, France, 2001.

X. Huang, B.W. Reinisch, D. Bilitza and R. Benson. New Data Source for Studying and Modelling the Topside Ionosphere. American Geophysical Union (AGU) 2001 Spring Meeting, May 29-June 2, 2001, Boston, MA (2001): SA61A-10.

X. Huang, B. W. Reinisch, D. Bilitza and R. F. Benson, New Data on the Topside Electron Density Distribution, International Beacon Symposium, Boston College, Massachusetts, June 3-6, 2001.

D. Bilitza, B. Reinisch, R. Benson, J. Grebowsky, N. Papitashvili, X. Huang, W. Schar, and K. Hills, Online data base of satellite sounder and insitu measurements covering two solar cycles, IRI Workshop, INPE, Brazil, 2001.

D. Bilitza, Bodo Reinisch, and Xueqin Huang, Automated Processing of ISIS Topside Ionograms into Electron Density Profiles, Oct 2001.

D. Bilitza, X. Huang, B. W. Reinisch, and R. F. Benson, TOPIST – AUTOMATED PROCESSING OF ISIS TOPSIDE IONOGRAMS, Ionospheric Effects Symposium, Alexandria, Virginia, 2002.

D. Bilitza, K. Hills, B. Reinisch, X. Huang, R. Benson, and W. Schar, The ISIS Topside Sounder Data Save and Rescue Effort, Raytheon Data Center Symposium, Landover, Maryland, 2003.

## APPENDIX E: Papers published

Bilitza, D., ISIS Team Meets at NSSDC to Discuss Density Profile Generation, NSSDC Newsletter, March 2001.

Bilitza, D., Density Profiles from the Alouette 1, 2 and ISIS 1, 2 Topside Sounder Instrument on CD-ROM and WWW. In: S.M. Radicella, Ed., *Proceedings of the IRI Task Force Activity 2000, July 10-14, 2001, Trieste, Italy*, Abdus Salam International Center for Theoretical Physics (ICTP), Report IC/IR/2001/7, Trieste, Italy, 2001.

Bilitza, D., Density Profiles from the Alouette 1, 2 and ISIS 1, 2 Topside Sounder Instrument on CD-ROM and WWW, International Reference Ionosphere Newsletter, pp. 8-14, Volume 8, No. 1/2, June 2001.

Huang X., B. Reinisch, D. Bilitza, and R. Benson, Electron density profiles of the topside ionosphere, *Annals Geophys.* 45, #1, 125-130, 2002.

Bilitza, D., ISIS Topside Sounder Data available online at NSSDC, AGU SPA Newsletter, Dec 2002.

Huang X., B. Reinisch, D. Bilitza, and R. Benson, New Data on the Topside Electron Density Distribution, *Proceedings of 2001 Beacon Symposium*, Boston University, 2002.

Bilitza, D., B. Reinisch, R. Benson, J. Grebowsky, N. Papitashvili, X. Huang, W. Schar, and K. Hills, Online data base of satellite sounder and insitu measurements covering two solar cycles, *Adv. Space Res.* 31, #3, 769-774, 2003.

Bilitza, D., X. Huang, B. Reinisch, R. Benson, H.K. Hills, W.B. Schar, Topside Ionogram Scaler With True Height Algorithm (TOPIST): Automated processing of ISIS topside ionograms, *Radio Sci.*, Vol. 39, No. 1, RS1S27 10.1029/2002RS002840 16 January 2004

Bilitza, D., A correction for the IRI topside electron density model based on Alouette/ISIS topside sounder data, *Adv. Space Res.* 33, #6, 838-843, 2004.